

DISSERTATIONES CHIMICAE UNIVERSITATIS TARTUENSIS

62

**ELECTROREDUCTION
OF PEROXODISULFATE ANION ON
BISMUTH ELECTRODES**

RUTHA JÄGER



TARTU UNIVERSITY
PRESS

Department of Chemistry, Institute of Physical Chemistry, University of Tartu,
Estonia

Dissertation in physical and electrochemistry

Dissertation is accepted for the commencement of the degree of Doctor of Philosophy in Chemistry on March 6, 2007, by the Doctoral Committee of the Department of Chemistry, University of Tartu.

Supervisor: Prof. Enn Lust

Opponents: Prof. Oleg. A. Petrii (M.V. Lomonosov Moscow State
University)
Prof. Emer. Vello Past (University of Tartu)

Commencement: April 27, 2007 at 18 Ülikooli Str., room 204, 14:00 h.

ISSN 1406-0299
ISBN 978-9949-11-558-7 (trükis)
ISBN 978-9949-11-559-4 (PDF)

Autoriõigus Rutha Jäger, 2007

Tartu Ülikooli Kirjastus
www.tyk.ee
Tellimuse nr. 83

In memory of my grandmother

CONTENTS

1. LIST OF ORIGINAL PUBLICATIONS.....	8
2. ABBREVIATIONS AND SYMBOLS.....	9
3. INTRODUCTION	11
4. CALCULATION OF KINETIC PARAMETERS.....	13
5. EXPERIMENTAL.....	16
6. RESULTS AND DISCUSSION	19
6.1 Cyclic and rotating disc electrode voltammetry data for electroreduction of the peroxodisulfate anion at Bi(<i>hkl</i>)	19
6.2 Kinetic analysis	25
6.3 Corrected Tafel plots	30
7. CONCLUSIONS	48
8. REFERENCES	49
9. SUMMARY IN ESTONIAN Peroksodisulfaataniooni elektrokeemiline redutseerumine Bi elektroodil.....	52
10. ACKNOWLEDGMENTS	53
11. PUBLICATIONS.....	55

1. LIST OF ORIGINAL PUBLICATIONS

The present thesis consists of the five articles listed below.

1. E. Lust, **R. Truu** and K. Lust, Electroreduction of peroxodisulfate anion at Bi(111) single-crystal electrode, Russian J. of Electrochemistry, 36 (2000) 1195–1202.
2. **R. Jäger**, E. Härk, P. Möller, J. Nerut, K. Lust and E. Lust, The kinetics of electroreduction of hexaamminecobalt(III) cation on Bi planes in aqueous HClO₄ solutions, J. Electroanal. Chem. 566 (2004) 217–226.
3. T. Thomberg, J. Nerut, **R. Jäger**, P. Möller, K. Lust, E. Lust, The kinetics of electroreduction of peroxodisulfate ions on single crystal cadmium and bismuth electrodes, J. Electroanal. Chem. 582 (2005) 130–143.
4. E. Lust, J. Nerut, E. Härk, S. Kallip, V. Grozovski, T. Thomberg, **R. Jäger**, K. Lust, K. Tähnas, Electroreduction of complex ions at bismuth and cadmium single crystal plane electrodes, ECS Transactions, 1 (17) (2006) 9.
5. **R. Jäger**, K. Lust, S. Kallip, V. Grozovski, E. Lust, Influence of surface nanoroughness of Bi electrodes on the electroreduction kinetics of S₂O₈²⁻ anion, J. Solid State Electrochem. (in press)

Author's contribution

- Publication 1:** The author performed all experimental work and is responsible for the data sets, calculations, preparation of manuscript.
- Publication 2:** The author made all experiments and calculations, which were made at Bi(01 $\bar{1}$) electrode. The author is responsible this part of manuscript, which described electroreduction of hexaamminecobalt(III) cation on Bi(01 $\bar{1}$) plane in aqueous HClO₄ solutions.
- Publication 3:** The author performed all experimental work at Bi(*hkl*) electrodes and is responsible for the data sets, calculations, preparation of this part of manuscript.
- Publication 4:** The author is responsible for the results, which describe electroreduction of peroxodisulfate anion on Bi(*hkl*) electrodes and electroreduction of hexaamminecobalt(III) cation on Bi(01 $\bar{1}$) plane in aqueous HClO₄ solutions.
- Publication 5:** The author is responsible for all voltammetry data sets, calculations and preparation of manuscript.

2. ABBREVIATIONS AND SYMBOLS

a	—	distance of the closest approach of various ions
A	—	constant characterising the permittivity of a solvent ($A = \sqrt{2\varepsilon\varepsilon_0RT}$)
C	—	differential capacitance
CHE	—	chemically etched electrode
c_i	—	bulk concentration of the discharging ion
$c_{\text{base el.}}$	—	base electrolyte concentration
cTp	—	corrected Tafel plot
D	—	diffusion coefficient
E	—	electrode potential
$E_{\sigma=0}$	—	zero charge potential
EP	—	electrochemically polished electrode
e_0	—	elementary charge
edl	—	electrical double layer
F	—	Faraday constant
f_0	—	activity coefficient
GCSG	—	Gouy-Chapman-Stern-Grahame model
(hkl)	—	notation of the crystallographic index
j	—	current density
j_d	—	limiting diffusion current density
j_k	—	kinetic current density
K_A	—	association constant
k_{cor}	—	rate constant corrected for the double layer effect
k_{het}	—	apparent rate constant of the heterogeneous reaction
k_0	—	potential independent rate constant
N_A	—	Avogadro constant
n_i	—	number of electrons consumed in the reaction of the ion
R	—	universal gas constant
SHE	—	standard hydrogen electrode
T	—	absolute temperature
x	—	distance of the reaction site from the outer Helmholtz plane
x_i	—	location of the effective point charge at a certain distance
z_{eff}	—	effective charge number of a reactant ion
z_i	—	charge number of a reactant ion
4M CE	—	calomel electrode in 4 M KCl
α	—	transfer coefficient
α_{app}	—	apparent transfer coefficient
ε	—	dielectric constant of the solvent

ϵ_0	—	dielectric constant of the vacuum
κ	—	Gouy screening length (i.e. the inverse Debye length)
ν	—	rotation velocity
ν	—	kinematic viscosity
σ	—	surface charge density
ψ_0	—	potential drop in the diffuse layer (outer Helmholtz plane potential)
ψ_1	—	electrical potential at the optimum point, where the charge transfer from metal to ion take place
ω	—	angular frequency ($\omega = 2\pi\nu$)

3. INTRODUCTION

Electroreduction of the $[\text{Co}(\text{NH}_3)_6]^{3+}$ and $\text{S}_2\text{O}_8^{2-}$ ions has been suggested as the model reactions to study the influence of the electric double layer characteristics on the charge transfer mechanism from metal to the complex ion [1,2]. Comparison of the results obtained by Hamelin and Weaver [1] with those obtained by Hromadova and Fawcett [2] shows that the rate constant values of the heterogeneous reactions of ions depend on the crystallographic structure of Au (*hkl*) surface, as well as on the chemical composition of the base electrolyte used. Electroreduction of peroxodisulfate anion on Au electrodes has been suggested to proceed via two parallel pathways [3–6] and Samec et al. have demonstrated that the first pathway gives rise in a current at positively charged polycrystalline Au, Au(111) and Au(011) electrodes and involves a stronger interaction of the discharging $\text{S}_2\text{O}_8^{2-}$ anion with the electrode surface resulting in an electrocatalysis of this process. However, a direct electroreduction (i.e. classical Frumkin mechanism [7–9]) of the $\text{S}_2\text{O}_8^{2-}$ anions at more negative potentials for Au electrodes has been observed. A dynamic model of a $\text{S}_2\text{O}_8^{2-}$ electrochemical oscillator was put forward, which refers to conclusions derived from studies of peroxodisulfate reduction on Hg [3–6].

Quantum chemical simulations and the future development of charge transfer mechanism have been discussed in Refs. [10,11]. The strong influence of the surface structure and chemical nature of Cd(*hklf*) electrode on the $\text{S}_2\text{O}_8^{2-}$ electroreduction kinetics has been established using the cyclic voltammetry and rotating disk electrode methods [12–15]. It was found that, in case of more hydrophilic Cd(0001) plane in the limited region of the base electrolyte concentrations ($1 \times 10^{-3} \text{ M} < c_{\text{NaF}} < 2 \times 10^{-2} \text{ M}$), the kinetics of electroreduction of the $\text{S}_2\text{O}_8^{2-}$ anions, to a first approximation, can be simulated by the Frumkin slow discharge theory [7–9,16,17].

The main aim of this work is to study the influence of the surface crystallographic structure of Bi electrodes on the charge transfer mechanism and kinetic characteristics of electroreduction of $\text{S}_2\text{O}_8^{2-}$ anions to SO_4^{2-} anions and compare the data obtained with the corresponding data of electroreduction of $[\text{Co}(\text{NH}_3)_6]^{3+}$ cations at Bi(*hkl*). According to the data of various investigators [1,2,18–21], electroreduction of the $[\text{Co}(\text{NH}_3)_6]^{3+}$ cations has been suggested as a “model adiabatic outer-sphere” reaction and, therefore, it would give us the possibility to examine the influence of the electrical double layer (edl) structure (i.e. dependence of edl and diffuse layer potential drop (electrostatic work term) on the electrode material) on the electrochemical parameters for the electro-

reduction process at the Bi planes. The electroreduction of $\text{S}_2\text{O}_8^{2-}$ anions belongs to the group of reaction with the complicated mechanism taking into account that the chemical bond breaks irreversible.

4. CALCULATION OF KINETIC PARAMETERS

Experimental data for various polycrystalline sp-metals like Bi, Sb, Pb, Sn, Hg(Cu) Cd, In, Tl and Ag [9,17,22–26], as well as for single-crystal Ag(111) and Ag(100) planes [27–29] have implied that the rate of the overall two-electron peroxydisulfate reduction is controlled by a single one electron rate-determining step. This rate-determining step can be characterised by an apparent heterogeneous rate constant k_{het} value, expressed as

$$k_{het} = k_{cor} \exp(-z_i F \psi_1 / RT) = k_0 \exp(-z_i F \psi_1 / RT) \exp[-\alpha F(E - \psi_1) / RT] \quad (1)$$

where k_{cor} is the rate constant corrected for double layer effect (so-called Frumkin correction (ψ_1 effect)); ψ_1 is the electrical potential at the optimum point, where charge transfer from metal to ion takes place; z_i is the charge number of a reactant ion, α is the transfer coefficient; and k_0 is the potential-independent rate constant. It should be noted that in the case of $S_2O_8^{2-}$ the electroreduction is irreversible due to breaking of the oxygen-oxygen bond [8,14,17,22,23,30–32]. As shown in Refs. [9,17,22–26,33–37] and noted by Samec, Doblhofer et al. [3–5], this picture is oversimplified even for Hg electrode [7,8,10,11]. It is to be noted, that the very low α values ($\alpha = 0.22$ if $z = -2$) have been reported [17,22,23,26], and according to Gierst [33] α depends on the electrode potential. Results of quantum chemical calculations [38,39] shows that the electroreduction of the $S_2O_8^{2-}$ anion belongs to the group of the reactions with a very complicated mechanism and the transfer of the first electron to the $S_2O_8^{2-}$ anion takes place according to the following equation



It was found that the transfer of the first electron is probably the rate determining step and the standard potential for the redox couple $E_{S_2O_8^{2-}/SO_4^{2-};SO_4^{\bullet-}}^0 = 1.45$ V versus SHE [38–42]. According to the experimental results, there is no specific adsorption of the $S_2O_8^{2-}$ anions on the Hg electrode and the reaction centre lies in the diffuse layer [5,14,17,22–24,27,29,38,42,43]. The very low values of α_{app} for the Hg electrode have been explained theoretically by Petrii and co-workers [7,38,39] by the diabatic and activationless charge transfer mechanism [30,32].

It should to be noted that Damaskin et al. [8] have discussed the possibility to use the new diffuse layer theory developed by Gonzalez and Sanz [44] where the activity of the $S_2O_8^{2-}$ anions at the outer Helmholtz plane has been used as the concentration variable to construct the so-called corrected Tafel plots (cTp) [45]. It was found that for $K_2S_2O_8 + K_2SO_4$ system on Hg electrode the new model gives

reasonable results (with $\alpha_{app} = 0.11$) but for $K_2S_2O_8 + KF$ system the influence of the activity of the anions and corresponding corrections is very small [8].

According to the new so-called microscopic double layer ψ_i potential correction model [12,19,38,39,46–52], the interaction of reactants with the electrical double layer field can be modelled on the basis of the so-called “microscopic “ approach, taking into account the effective charges of the atoms forming the complex ions.

Another more usual representation is based on the location of the effective point charge at a certain distance x_i with subsequent calculation of the effective values z_{eff} [12,22,31,43,47–52]. In the papers published by Frumkin et al. [14,17,22,23,31,43] and Petrii et al. [53,54], there has been developed a formal conception taking into account that the ψ_i potential is different from the Gouy-Chapman diffuse layer potential ψ_0 for aqueous NaF base electrolyte solution and the effective double layer potential at the reaction site, $\psi_x(x_i)$, has been calculated as [19,45]

$$\psi_x(x_i) = \frac{4RT}{F} \arctan h \left\{ \tanh \left(\frac{F\psi_0}{4RT} \right) \exp[-\kappa(x_i - x_d)] \right\}, \quad (3)$$

where κ is the Gouy screening length (i.e. the inverse Debye length) for the electrolyte solution with concentration c and κ expressed as

$$\kappa = \left(\sqrt{\frac{\varepsilon_0 \varepsilon RT}{2cF^2}} \right)^{-1}. \quad (4)$$

where ε is the dielectric constant of solvent and ε_0 is dielectric constant of vacuum. In Eq. (3) ψ_0 is the classical Gouy-Chapman diffuse layer potential for the base electrolyte and according to the Gouy-Chapman theory ψ_0 potential for symmetrical z,z -electrolyte has expressed as

$$\psi_0 = \frac{2RT}{|z|F} \arcsin \left[\frac{\sigma}{2A\sqrt{c}} \right] \quad (5)$$

where σ is the surface density and $A = (2\varepsilon_0 \varepsilon RT)^{-1/2}$. In Eq. (3), the variable $x = (x_i - x_d)$ is a distance of reaction site from the outer Helmholtz plane with distance x_d from the electrode surface and the potential drops linearly from the value of ϕ_m at the interface to the value ψ_0 at the outer Helmholtz plane $\left(\psi_x(x_i) = \phi_m - (\phi_m - \psi_0) \frac{x_i}{x_d} \right)$ if reaction site lies in the inner layer region [19].

For electroreduction of the $S_2O_8^{2-}$ anion on Hg, it was found that the linear corrected Tafel plots can be established if the reaction site is assumed to lie in

the inner layer, i.e., at the distance somewhat smaller than the parameter of the effective ellipsoid formed by the $\text{S}_2\text{O}_8^{2-}$ anion (0.32 and 0.68 nm, respectively) [19,22,38,39,46,54]. However, for electroreduction of $[\text{Fe}(\text{CN})_6]^{3-}$ ions on Hg very large values of the distance from the outer Helmholtz plane, x , have been established (i.e., $x \geq 1.0$ nm) [14,17,53–55] and according to these data this distance is more than two times larger than the effective diameter of the $[\text{Fe}(\text{CN})_6]^{3-}$ ion (equal to 0.41 nm) [51]. Thus, the double layer correction for electroreduction of the complex anions at the so-called Hg-like metals in various base electrolyte solutions is an open question.

5. EXPERIMENTAL

A conventional three-electrode jacketed glass cell was used for all electrochemical studies. The electrochemically polished (EP) single crystal Bi(111) and Bi(01 $\bar{1}$) planes were used as the working electrodes. These electrodes were prepared according to the methods described in Refs. [56–58]. The cleanliness of the base electrolyte solution and the quality of the electrode surface were verified by cyclic voltammetry and impedance methods as well as by *in situ* STM (Figs. 1 and 2) [59], AFM, X-ray diffraction and electron microscopy studies. In addition to electrochemically polished Bi(111) electrodes the chemically etched (with HNO₃) Bi(111) plane (Fig. 3) were used to study influence of surface nanoroughness on the electroreduction kinetics of peroxodisulfate anions [56–61].

A calomel reference electrode, filled with 4.0 M KCl solution, and a large Pt counter electrode completed the three-electrode setup. The reference electrode was connected to the cell through a long Luggin capillary filled with the same base electrolyte solution studied. The experiments were carried out at a temperature $T = 298$ K under pure argon atmosphere (99.999%). All solutions were prepared using nanopure water with resistivity ≥ 18.2 M Ω cm [56]. Glassware was cleaned with a hot H₂SO₄ + H₂O₂ mixture and rinsed with MilliQ+ water before each set of experiments. Solutions were prepared from triply recrystallised from the MilliQ+ water NaF, Na₂SO₄ and Na₂S₂O₈ salts. HClO₄, NaClO₄ and [Co(NH₃)₆]Cl₃ (all “Aldrich”) were of the best quality available. [Co(NH₃)₆](ClO₄)₃ was prepared from the corresponding chloride by precipitation with saturated sodium perchlorate and triply recrystallisation from water [1,2].

Cyclic voltammograms (CVs) (scan rate from 5 to 200 mV s⁻¹) and rotating disc voltammograms (scan rate from 5 to 20 mV s⁻¹ and rotation velocity $v = 0 \dots 9990$ rev min⁻¹) were obtained with the “Pine” rotating ring-disc electrode system.

For the accurate determination of the precision of the experimental data, a statistical treatment of the results was carried out. A total number of the independent experiments $n \geq 4$, and at least two different electrodes with same crystallographic orientation were used [60]. The relative error of current density at the constant electrode potential (E) was not more than 5–10%.

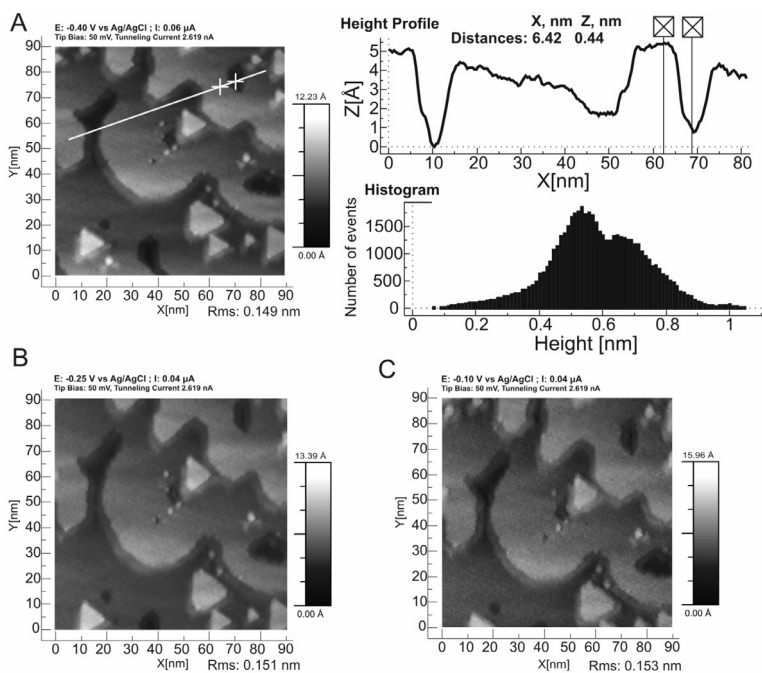


Fig. 1. *In situ* STM images at various electrode potentials (shown in A, B and C) for electrochemically polished Bi(111) electrode in 0.0001 M HClO₄ + 0.0099 M LiClO₄ aqueous solution; selected surface profile and histogram of the height distribution for (A).

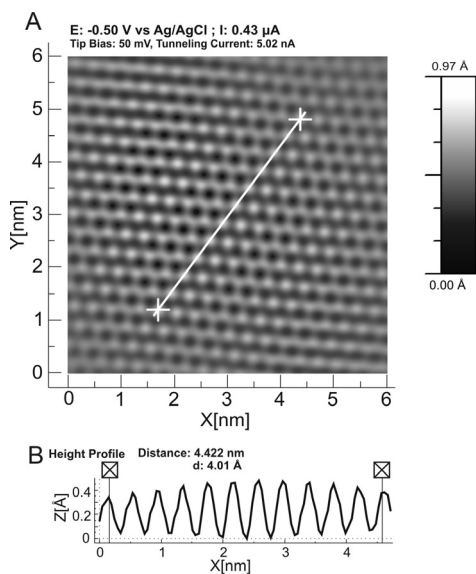


Fig. 2. *In situ* atomic resolution STM image (A) and height profile (B) for Bi(111) electrode at $E = -0.5$ V vs Ag/AgCl in 5×10^{-2} M Na₂SO₄ + 5×10^{-4} M H₂SO₄ aqueous solution.

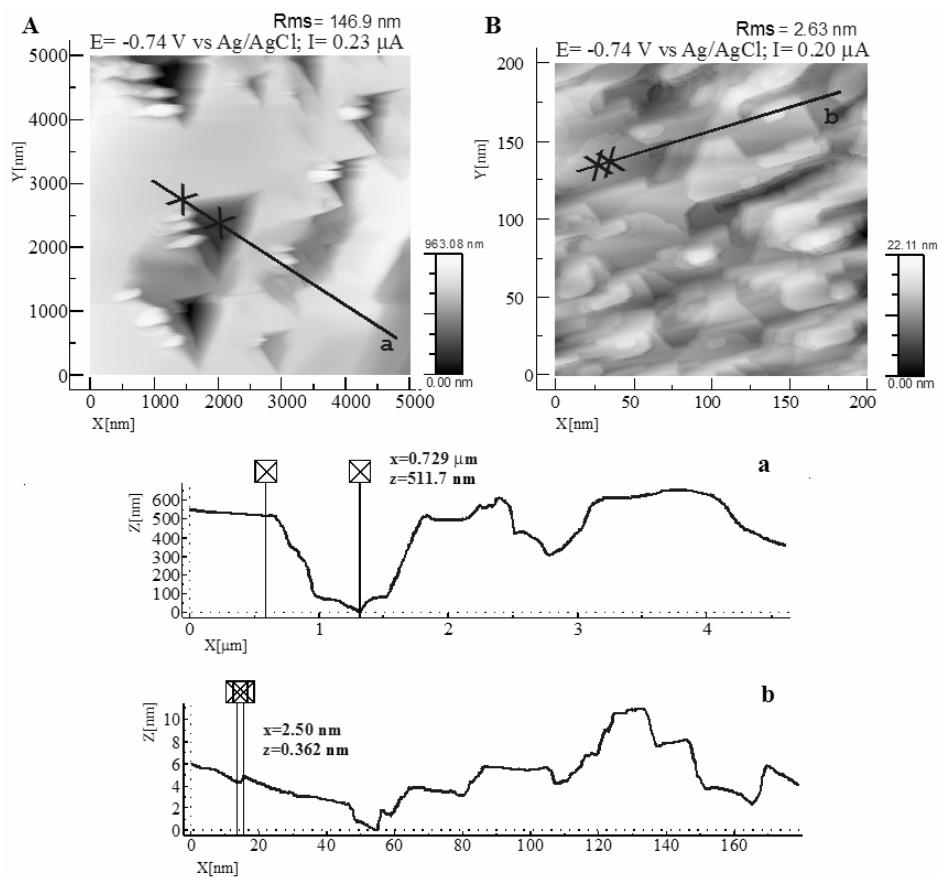


Fig. 3. The *in situ* STM images of electrochemically polished Bi(111) electrode and thereafter chemically etched with concentrated HNO₃ (A,B) at $E = -0.74$ V vs Ag/AgCl in 0.5 M Na₂SO₄ + 3×10^{-4} M H₂SO₄ solution, selected height profiles (a) and (b).

6. RESULTS AND DISCUSSION

6.1. Cyclic and rotating disc electrode voltammetry data for electroreduction of peroxodisulfate anion at Bi(*hkl*)

The cyclic voltammograms of the peroxodisulfate anion (5×10^{-5} M $\text{Na}_2\text{S}_2\text{O}_8$ solution) electroreduction at Bi(111) in NaF solutions are displaced in Figs. 4–6.

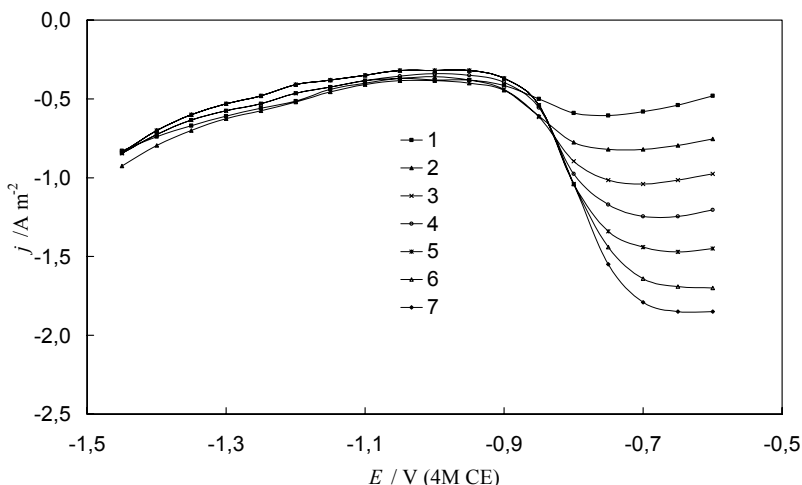


Fig. 4. Rotating disc voltammetry curves (scan rate 10 mV s^{-1}) for the EP Bi(111) plane in 5×10^{-5} M $\text{Na}_2\text{S}_2\text{O}_8 + 2 \times 10^{-3}$ M NaF solution at different rotation velocities v (rev min^{-1}): (1) 960, (2) 1900, (3) 3100, (4) 4600, (5) 6450, (6) 8600, (7) 9900.

According to these data, the rate of electroreduction of $\text{S}_2\text{O}_8^{2-}$ to SO_4^{2-} noticeably depends on the electrode potential, on the rotation velocity of electrode v and on the concentration of base electrolyte and peroxodisulfate anions in solution. Differently from Au electrodes [3–5], a hysteresis of current density between the negative and positive scan direction of potential in the region of mixed kinetics was not observed if $c_{\text{Na}_2\text{S}_2\text{O}_8} \leq 1 \times 10^{-4}$ M. Noticeable hysteresis was observed at $c_{\text{Na}_2\text{S}_2\text{O}_8} \geq 2 \times 10^{-4}$ M. As there is no hysteresis in the j, E curves for the pure base electrolyte solutions (NaF or Na_2SO_4), this effect is probably caused by the slow adsorption of anions (or intermediate product of the reaction) at Bi(*hkl*) electrode surface.

The dependence of the differential capacitance on the cation hydration energy in the region of the diffuse layer minimum potential $E_{\sigma=0}$ (C increases in the order $\text{LiF} < \text{NaF} < \text{KF}$) indicates the complicated cation coadsorption process caused by the weak specific adsorption of F^- anions near the zero charge

potential and by changes in the diffuse layer structure [7–9,22,61–66]. For that reason, all the kinetic data were calculated from the experimental j,E curves within the range $-1.6 \leq E \leq -0.5$ V (4M CE) for Bi(hkl). In the region of zero charge potential $-0.7 \text{V} \leq E \leq -0.6$ V (4M CE) for EP Bi(111) the very well exposed current plateaus were found, if base electrolyte concentration c_{NaF} is low or electrode rotation velocity v is small. If base electrolyte concentration rises then current plateaus shift towards less negative potentials. The same effect takes place if electrode rotation velocity rises.

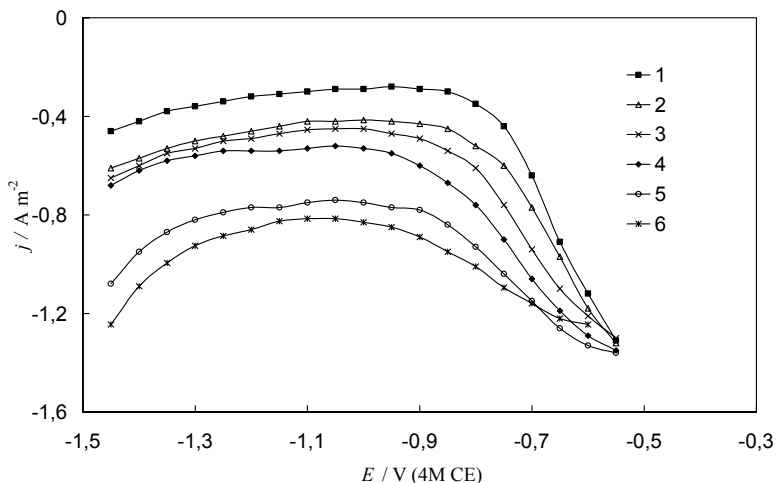


Fig. 5. Rotating disc voltammetry curves (scan rate 10 mV s^{-1} ; rotation velocity $v = 7500 \text{ rev min}^{-1}$) for the EP Bi(111) plane in $5 \times 10^{-5} \text{ M Na}_2\text{S}_2\text{O}_8$ solution with different additions of the base electrolyte NaF (M): (1) 0.003, (2) 0.005, (3) 0.007, (4) 0.01, (5) 0.02, (6) 0.03.

According to the data in Fig. 5 coincidence of experimental j,E curves takes place at $E_{\sigma=0}$ for Bi(111). For $c_{\text{NaF}} > 3 \times 10^{-2} \text{ M}$ and at $E > -0.8 \text{ V}$, the experimental current density values decrease with the rise of c_{NaF} in solution, caused by the weak adsorption of F^- anions [57,58]. However the current density values (j) at $E = \text{const.}$ were found to fit very well to the Levich ($j, \omega^{1/2}$) plot ($0.997 \leq R^2 \leq 0.999$) if $c_{\text{NaF}} < 3 \times 10^{-2} \text{ M}$. According to Refs. [17,22,37], the limiting diffusion current should follow the Levich equation [30]

$$j_d = 0.620 n_i F v^{-1/6} D^{2/3} \omega^{1/2} c_i \quad (6)$$

where n_i is the number of electrons consumed in the reaction; c_i is the concentration of the discharging ion in the bulk of solution; v is the kinematic viscosity; D is the diffusion coefficient and ω is the angular frequency ($\omega = 2\pi v$, where v is electrode rotation velocity). Taking $n_i = 2$ and $v = 0.01 \text{ cm}^2 \text{ s}^{-1}$, the diffusion coefficient of peroxodisulfate anion ($D = 9.5 \times 10^{-6} \text{ cm}^2 \text{ s}^{-1}$ for $2 \times 10^{-3} \text{ M}$

NaF) in a good agreement with literature data [3–5,22–26,61,67–69] has been calculated. Thus, in this region of potentials, the electroreduction of $S_2O_8^{2-}$ anion on EP Bi(111) plane is mainly limited by the rate of diffusion of $S_2O_8^{2-}$ to the electrode surface if $c_{NaF} < 3 \times 10^{-2}$ M. It should be noted that for more concentrated base electrolyte solutions ($c_{NaF} > 3 \times 10^{-2}$ M) the current densities are lower than the limiting diffusion currents at EP Bi(111) at $-0.7V \leq E \leq -0.6V$ (4M CE) and if we compared with CHE Bi(111) or EP Bi(01 $\bar{1}$) planes, current plateaus at $-0.7V \leq E \leq -0.6V$ (4M CE) only for the very dilute NaF solutions ($c_{NaF} \leq 0.002$ M) have been found [69]. This effect can be explained by the more active and defect surface structure of CHE Bi(111) electrode and by more remarkable adsorption of the $S_2O_8^{2-}$ ions (or reaction intermediates) and co-adsorption of Na^+ ions [7–9,14,17,22–24,31,43,47] followed by formation of the $Na^+S_2O_8^{2-}$ ion pairs in the inner layer region of the electrical double layer. Thus, the so-called “surface blocking effect”, caused by adsorption of the reaction intermediates or reactants, more remarkable for CHE Bi(111) than for EP Bi(111), has been observed [68,69].

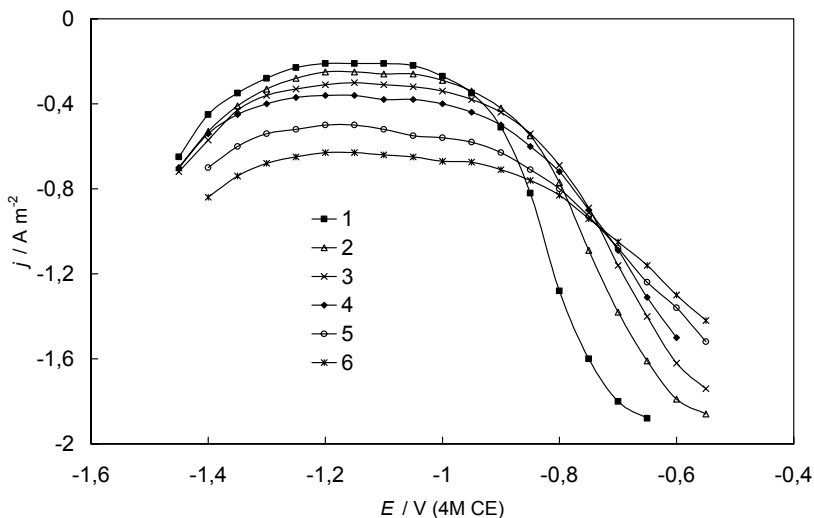


Fig. 6. Rotating disc voltammetry curves (scan rate 10 mV s^{-1} ; rotation velocity $v = 7500 \text{ rev min}^{-1}$) for the CHE Bi(111) plane in 5×10^{-5} M $Na_2S_2O_8$ solution with different additions of the base electrolyte NaF (M): (1) 0.003, (2) 0.005, (3) 0.007, (4) 0.01, (5) 0.02, (6) 0.03.

According to Figs. 4–7, with the rise of negative polarisation ($E \leq -0.7V$ (4M CE)) the inhibition of peroxodisulfate anion electroreduction begins, caused by the rise of negative value of ψ_1 potential as well as by repulsion of the negatively charged

$S_2O_8^{2-}$ anions from electrode surface. In dilute base electrolyte solutions a cathodic minimum of current density at $-1.1V \leq E \leq -0.9V$ (4M CE) has been found for EP Bi(*hkl*) plane. E_{cat} (potential of cathodic minimum in j, E -curves) somewhat depends on the concentration of base electrolyte (Figs. 5, 6 and 7) and with the rise of $c_{base\ electrolyte}$ the value of E_{cat} shifts towards more negative potentials. Thus, with the decrease of absolute value of diffuse layer potential $|\psi_0|$ (i.e, with decrease of electrostatic work), the value of E_{cat} shifts towards more negative surface charge densities. In comparison with Cd(0001) electrode [9–11] the cathodic current density minimum has been observed at noticeably less negative potential, which is caused by the differences in the zero charge potential values for Bi(*hkl*) and Cd(0001) [70,71]. It should be mentioned that for Cd(0001) $E_{\sigma=0} = -0.97V$, but for Bi(111) $E_{\sigma=0} = -0.66V$ (vs 4M CE). Differently from Cd(0001), there is no noticeable dependence of current density on the rotating speed of the Bi(*hkl*) electrode (Fig. 4). Thus the nearly pure kinetic current densities have been observed for Bi(*hkl*) at $-1.25V < E < -0.9V$ (4M CE).

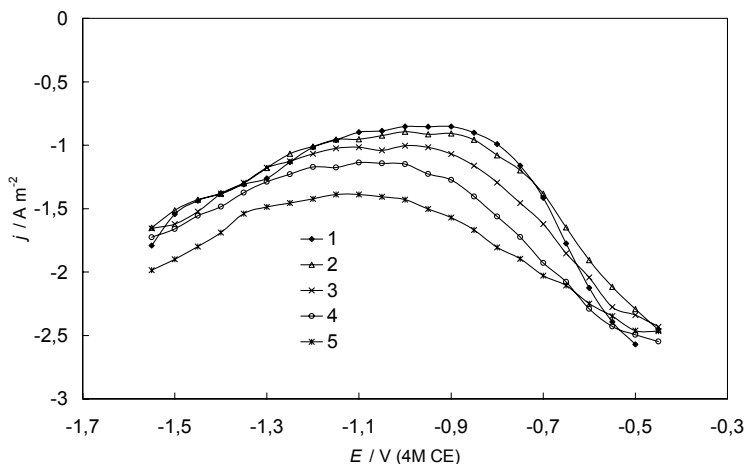


Fig. 7. Rotating disc voltammetry curves (scan rate 10 mV s^{-1} ; $\nu = 7000\text{ rev min}^{-1}$) for the EP Bi($01\bar{1}$) plane in $1 \times 10^{-4}\text{ M Na}_2\text{S}_2\text{O}_8$ solution with different additions of the base electrolyte Na_2SO_4 (M): (1) 0.003, (2) 0.005, (3) 0.007, (4) 0.01, (5) 0.02.

At more negative surface charge densities ($E \leq -1.2V$ (4M CE)) acceleration of $S_2O_8^{2-}$ anion electroreduction occurs and in this region $d\psi_1/dE \approx const.$ [56–58,60,61,68–71]. Acceleration of reaction is mainly caused by the decrease of electrode potential, as well as by beginning the electrostatic adsorption of base electrolyte cations at the negatively charged Bi electrode surface. This result is in a good agreement with the impedance data as in this region of potentials $E \leq -1.3V$ (vs. 4M CE)) the weak rise of capacitance values with c_{NaF} and $c_{Na_2S_2O_8}$ for Bi(*hkl*) planes was observed [57–58,61,68–71]. It should be noted

that the values of differential capacitance in the 0.1 M NaF solution are higher than those in LiClO₄ solution ($\Delta C \sim 1.0 \mu\text{F cm}^{-2}$), demonstrating that very weak specific adsorption of the Na⁺ ions is possible on Bi(*hkl*) at $E \leq -1.5\text{V}$ (4M CE). Thus, at very negatively charged Bi(*hkl*) surface the exchange of the electroreduction mechanism of S₂O₈²⁻ anions is possible, i.e., additionally to the usual transfer process the simultaneous charge transfer through the adsorbed ion-pairs is probable. However, it should be noted that the very slow cathodic hydrogen evolution is also possible at $E \leq -1.5\text{V}$ (4M CE). The rise in cathodic current densities is lower for Bi(*hkl*) planes, which is mainly caused by the higher hydrogen overvoltage for Bi(*hkl*) compared with Cd(0001) electrode [64,68–72]. Thus, at least two simultaneous cathodic processes seem to take place at very negative surface charge densities. The smaller increase in the cathodic current density for Bi(*hkl*) in comparison with Cd(0001) plane is mainly caused by more pronounced adsorption of the Na⁺ cations at Bi(*hkl*) at $\sigma \ll 0$ than at Cd(0001) plane [12,22,23,31,43,47,59,61–65,69–72]. It is to be noted that usually this region ($E < -1.6\text{V}$ (vs 4M CE)) was not studied in detail and therefore not used for the quantitative analysis of data.

The data in Fig. 8 show that there is a systematical decrease of the diffuse layer minimum potential ΔE_{min} values (b) in differential capacitance, electrode potential (C, E) curves (a), as well as increase of the differential capacitance values at E_{min} caused by the noticeable adsorption of S₂O₈²⁻ anions (or negatively charged reaction intermediates) at Bi(111) [56–60].

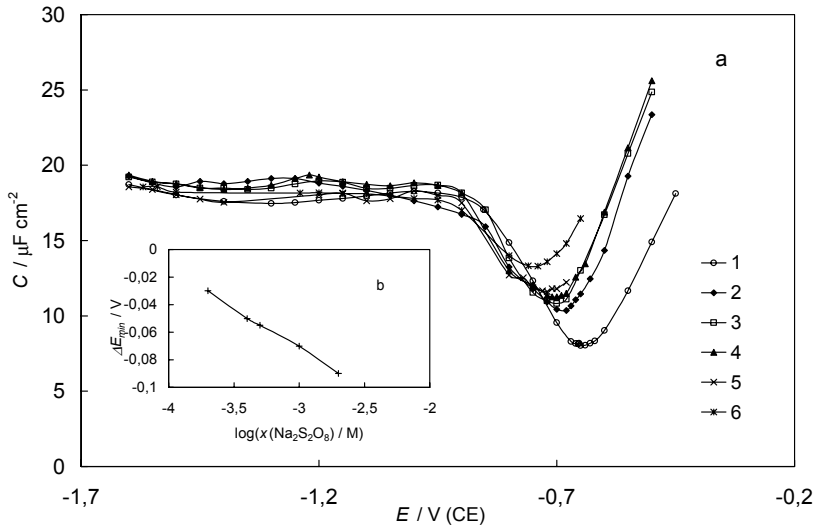


Fig. 8. Differential capacitance vs electrode potential curves for EP Bi(111) plane (a) in 0.001M NaF (1) and in 0.001M NaF + $x\text{M Na}_2\text{S}_2\text{O}_8$: (2) 2×10^{-4} , (3) 4×10^{-4} , (4) 5×10^{-4} , (5) 1×10^{-3} , (6) 2×10^{-3} ; and $\Delta E_{min}, \log c_{\text{Na}_2\text{S}_2\text{O}_8}$ dependences (b).

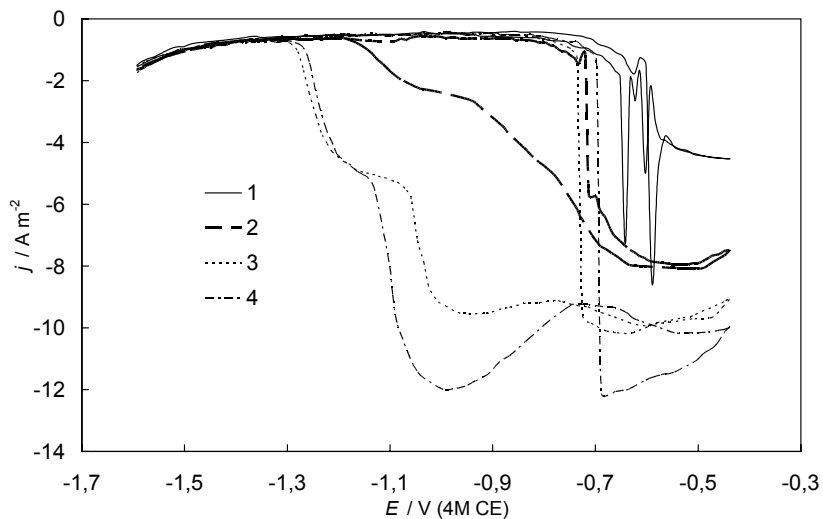


Fig. 9. Rotating disc voltammetry curves (scan rate 10 mV s^{-1}) for the EP Bi(01 $\bar{1}$) plane in $5 \times 10^{-4} \text{ M Na}_2\text{S}_2\text{O}_8 + 2 \times 10^{-3} \text{ M NaF}$ solution at different rotation velocities v (rev min^{-1}): (1) 1000, (2) 3000, (3) 5000, (4) 7000.

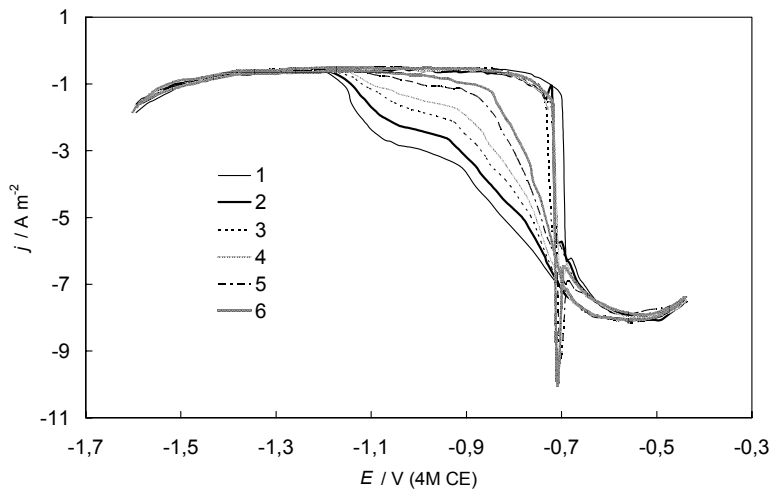


Fig. 10. Rotating disc voltammetry curves (rotation velocity $v = 3000 \text{ rev min}^{-1}$) for the EP Bi(01 $\bar{1}$) plane in $5 \times 10^{-4} \text{ M Na}_2\text{S}_2\text{O}_8 + 2 \times 10^{-3} \text{ M NaF}$ solution at different scan rates (mV s^{-1}): (1) 5, (2) 10, (3) 20, (4) 30, (5) 60, (6) 100.

Figs. 9 and 10 demonstrated the hysteresis of current density obtained between positive and negative going potential scans, were characteristic feature of j, E curves at $c_{\text{Na}_2\text{S}_2\text{O}_8} \geq 2 \times 10^{-4} \text{ M}$ can be seen. The hysteresis depends on rotation

velocity, potential scan rate, peroxydisulfate concentration and base electrolyte concentration in solution. The effect of the rotation velocity is illustrated in Fig. 9, which shows that the hysteresis increases with increasing of the electrode rotation velocity. It can be mention that at lower rotation velocity ($v \leq 3000 \text{ rev min}^{-1}$) the current density oscillations were found. When $v > 3000 \text{ rev min}^{-1}$ the oscillations do not exists, but the current density increase very quickly with the potential scan towards negative E . It can be caused by the specific adsorption of $\text{S}_2\text{O}_8^{2-}$ anions. At a constant rotation velocity (example $v = 3000 \text{ rev min}^{-1}$) the hysteresis increases with decrease of the potential scan rate ($100 - 5 \text{ mV s}^{-1}$). This effect can be explained by two parallel processes taking place in the region of mixed kinetics. Additionally to the slow charge transfer process the slow adsorption stage is probable. Differently from the region of mixed kinetics no dependence of current density or the potential scan rate was observed in the region of potentials ($E > -0.6\text{V}$ (vs 4M CE)), if rotation velocity is not too high. Thus, in this region of potentials, the electroreduction of the $\text{S}_2\text{O}_8^{2-}$ anion on the Bi (hkl) plane is mainly limited by the diffusion step of the electroactive $\text{S}_2\text{O}_8^{2-}$ anions to the electrode surface.

6.2. Kinetic analysis

The apparent rate constant of heterogeneous reaction of $\text{S}_2\text{O}_8^{2-}$ anions, k_{het} , was defined by the following equation

$$j_k = n_i F k_{het} c_i \quad (7)$$

where j_k is the kinetic current density; c_i is the bulk concentration of the discharging ion. The kinetic current density values at a constant potential have been obtained from the linear (so-called) Koutecky-Levich plots ($0.994 \leq R^2 \leq 0.999$) according to equation

$$1/j = 1/j_k + 1/j_d \quad (8)$$

where j is the experimental current density and j_d is diffusion current density. However, it is to be noted that the Eq. (8), at the first time, has been derived by Frumkin and Aikazian [73] and thereafter used by Frumkin and Tedoradze [74] for interpretation of experimental results.

The simple theory of the double layer effect on the apparent rate constant, developed by Frumkin et al. [14,17,22–26], predicts a sigmoidal dependence of the logarithm of the rate constant on the electrode potential. According to this theory, starting from positive surface charge densities and going towards negative values of E , $\log k_{het}$ first increases linearly with E . In the region of zero charge potential, $\log k_{het}$ begins to decrease as the value of $|\psi_1|$ potential increases ($\psi_1 \leq 0$). At higher negative surface charge densities, where $\partial\psi_1/\partial\sigma \approx const$ and

the influence of ψ_1 potential on $\log k_{het}$ values is small, $\log k_{het}$ again slowly increases with E according to the slow charge transfer theory of heterogeneous processes [14,17,22]. According to the theoretical conceptions [13–17], the magnitude of the potential drop to $\log k_{het}$ values should diminish when the electrolyte concentration increases and at very high electrolyte concentration a single linear dependence of $\log k_{het}$ on E would be seen ($\partial\psi_1/\partial E \approx 0$).

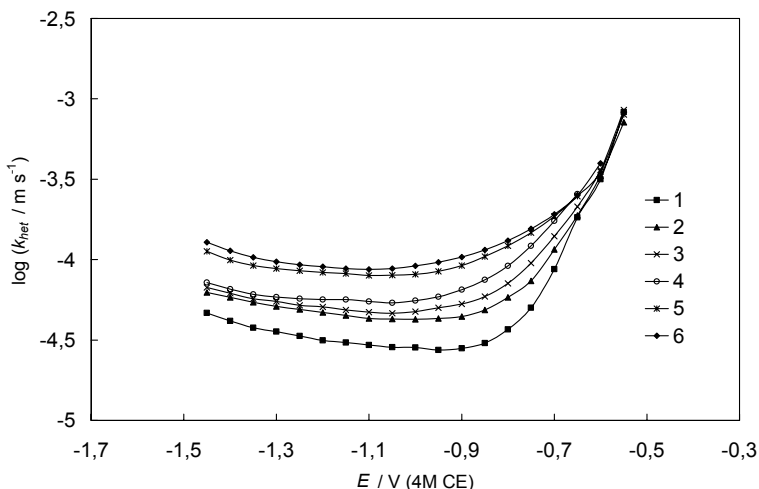


Fig. 11. $\log k_{het}$ - E - curves for EP Bi(111) plane in 5×10^{-5} M $\text{Na}_2\text{S}_2\text{O}_8$ solution with different additions of the base electrolyte NaF (M): (1) 0.003, (2) 0.005, (3) 0.007, (4) 0.01, (5) 0.02, (6) 0.03.

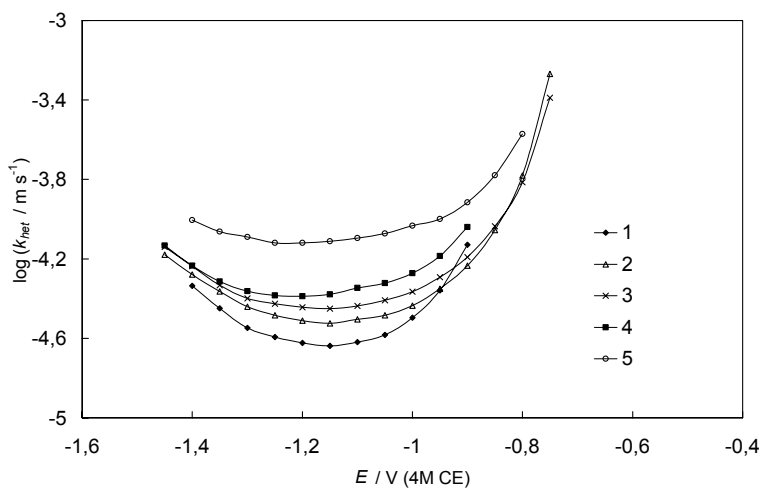


Fig. 12. $\log k_{het}$ - E - curves for CHE Bi(111) plane in 5×10^{-5} M $\text{Na}_2\text{S}_2\text{O}_8$ solution with different additions of the base electrolyte NaF (M): (1) 0.002, (2) 0.005, (3) 0.007, (4) 0.01, (5) 0.02.

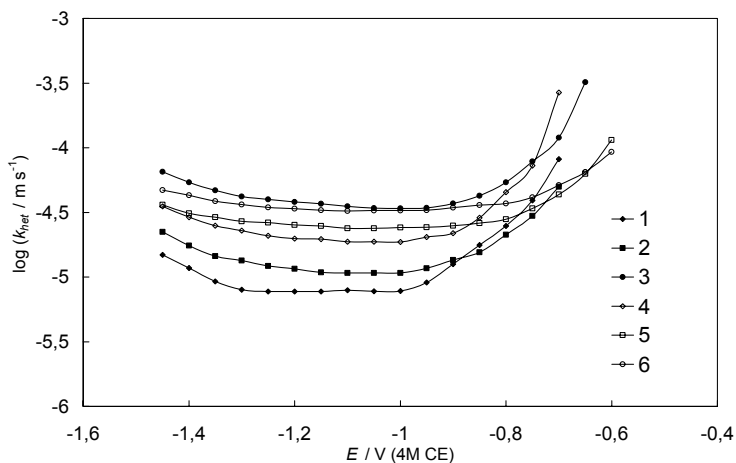


Fig. 13. Log k_{het} , E - curves for CHE Bi(111) plane (1–3) and for EP Bi(111) plane (4–6) in 1×10^{-4} M $\text{Na}_2\text{S}_2\text{O}_8$ solution with different additions of the base electrolyte NaF (M): (1,4) 0.003, (2,5) 0.007, (3,6) 0.02.

Figs. 11–13 demonstrate the statistically treated $\log k_{het}$, E dependences for Bi(111) electrodes. As it can be seen the values of $\log k_{het}$ (and j_k) decrease with dilution of the base electrolyte, but the decrease of k_{het} is somewhat smaller than that predicted according to the Frumkin slow charge transfer theory [13–17], especially for Bi(01 $\bar{1}$) plane (Fig. 14) at $E \ll E_{\sigma=0}$. The values of $\log k_{het}$ are somewhat higher for the EP Bi(111) plane compared with the data for CHE Bi(111) plane at $E \ll E_{\sigma=0}$, especially if $c_{\text{NaF}} < 1 \times 10^{-2}$ M (Fig 13). This effect is probably caused by the different activity of electrode surfaces investigated [56–58,61,68,69] explained by the higher nanoscopic surface roughness values for CHE Bi(111) compared with EP Bi(111) electrode (Figs. 1–3) [59]. However, for more concentrated solutions there are no differences in $\log k_{het}$ values for EP Bi(111) and CHE Bi(111) electrodes.

The values of j_k are somewhat higher for the Bi(111) plane (compared with Bi(01 $\bar{1}$)) and for Na_2SO_4 base electrolyte compared with NaF solutions (Fig. 14), which is in a good agreement with the higher ionic strength values for the 2:1 electrolyte system studied (Na_2SO_4) and with the Frumkin slow discharge theory [14,17,22,23,31,43].

Statistical analysis of the $\log k_{het}$, E plots shows that the values of $\log k_{het}$ decrease with increase of the reactant concentration $c_{\text{Na}_2\text{S}_2\text{O}_8}$ (Figs. 15 and 16), which indicates the weak adsorption of the reactant or reaction intermediates at the Bi(hkl) electrodes (i.e., the so-called surface blocking effect [4–6] has been established caused by the adsorption of the peroxodisulfate anions or reaction intermediates at the Bi(hkl) electrodes). Analysis of the $\log k_{het}$, E plots shows

that there are small dependences of $\log k_{het}$ on the reactant concentration only for more concentrated solutions ($c_{base\ electrolyte} \geq 0.02\text{ M}$). The values of k_{het} for Bi(*hkl*) planes are somewhat lower than those for Au(*hkl*) [4–6]. It should be mentioned that the value of k_{het} depends comparatively weakly on c_{NaF} as well as $c_{Na_2SO_4}$, which indicates the deviation of this experimental system from the simplified version of the Frumkin slow discharge theory [14,17,22–24,31,43] where the adsorption effects have been ignored.

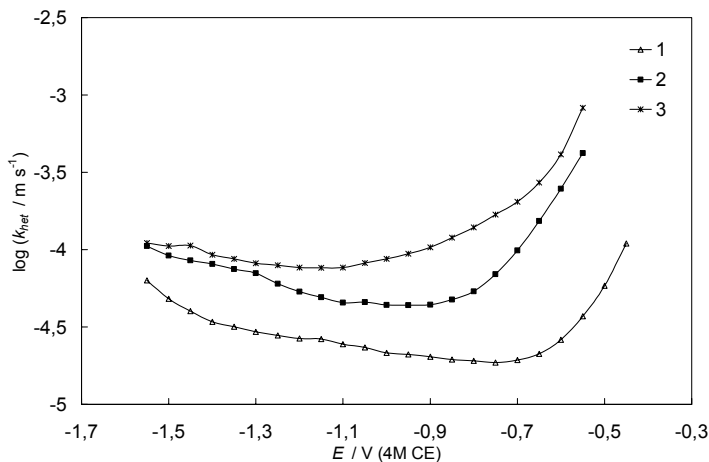


Fig. 14. $\log k_{het}$ - E - curves for EP Bi($01\bar{1}$) plane in 1×10^{-4} M $Na_2S_2O_8$ solution with additions of base electrolytes: (1) 0.02M NaF, (2) 0.003M Na_2SO_4 , (3) 0.02M Na_2SO_4 .

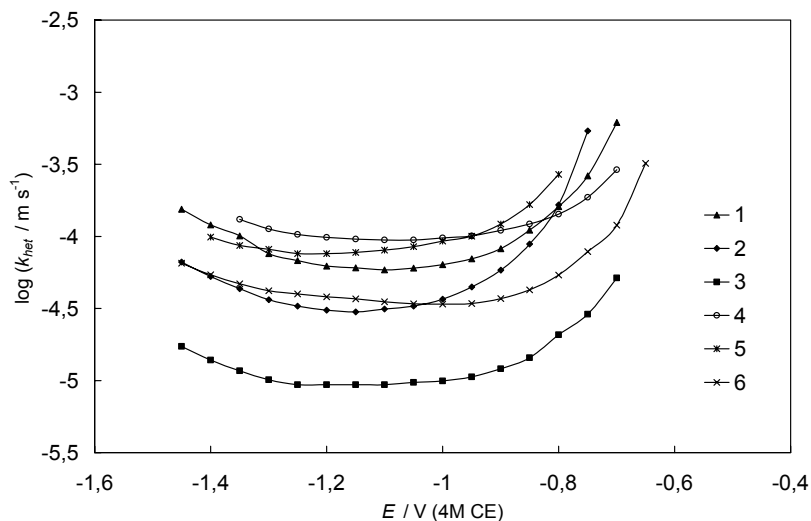


Fig. 15. $\log k_{het}$ - E - curves for CHE Bi(111) plane in 0.005M NaF (1–3) and in 0.02M NaF (4–6) with different additions of $Na_2S_2O_8$ (M): (1,4) 2×10^{-5} , (2,5) 5×10^{-5} , (3,6) 1×10^{-4} .

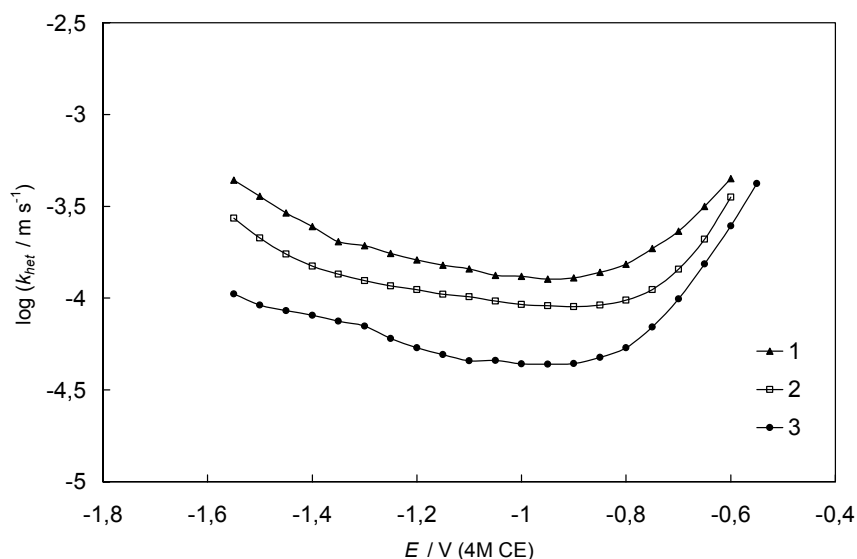


Fig. 16. Log k_{het} - E - curves for EP Bi(01 $\bar{1}$) plane in 0.003M Na₂SO₄ with different additions of Na₂S₂O₈ (M): (1) 2×10^{-5} , (2) 5×10^{-5} , (3) 1×10^{-4} .

Some experiments were made in solutions with addition of hydrochloric acid. Statistical analysis of the log k_{het} , E plots shows that the values of log k_{het} increase with addition of hydrochloric acid compared with system Na₂S₂O₈+NaF (Fig. 17). This effect can be explained by the specific adsorption of Cl⁻ anions at Bi(111) electrode and by the following shift of zero charge potential towards more negative E values and thus, by the decrease negative ψ_0 potential values and surface charge density values (by the decrease of the electrostatic work term) at fixed E . However, for more concentrated HCl solutions the noticeable cathodic hydrogen evolution takes place and the blocking effect of the electrode surface with the adsorbed H₂ bubbles is possible. For that reason these data have not been used for the quantitative analysis of reaction kinetics in this work.

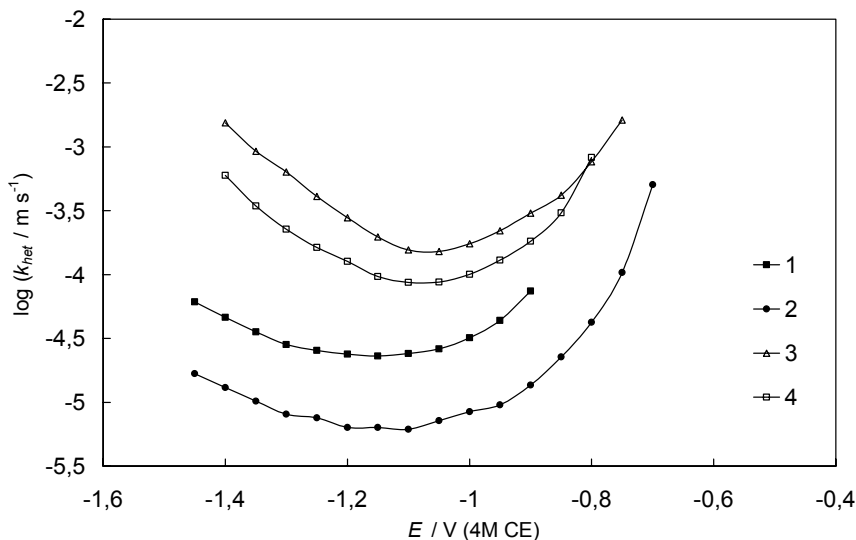


Fig. 17. Log k_{het} - E - curves for CHE Bi(111) plane in 0.002M NaF with different additions of $\text{Na}_2\text{S}_2\text{O}_8$ (M): (1) 5×10^{-5} , (2) 1×10^{-4} ; and in 0.002M NaF + 5×10^{-5} HCl with different additions of $\text{Na}_2\text{S}_2\text{O}_8$ (M): (3) 1×10^{-5} (4) 5×10^{-5} .

6.3. Corrected Tafel plots

The corrected Tafel plots (cTps) analysis method worked out by Delahay et. al [37,45] for the electroreduction of $\text{S}_2\text{O}_8^{2-}$ anion on Bi(hkl) electrode has been applied and the cTps have been calculated according to j_k values, obtained from linear $j^{-1}, \omega^{-1/2}$ -plots and using various empirical approximations for the ψ_1 potential values [7,8,12,14,17,22–24,30–32,38,39,43–52,67]. At first the classical Frumkin approximation was used (i.e., it was assumed that $\psi_1 = \psi_0$ and $z_i = -2$ for the anion, where ψ_0 is the potential at the outer Helmholtz plane and ψ_1 is the potential of the plane at which the centres of the charges of the reacting particles are located in the transition state of reaction). Comparison of the corrected Tafel plots for systems with $c_{\text{base electrolyte}} = \text{const.}$, but with different additions of $\text{S}_2\text{O}_8^{2-}$ anion, shows that the value of corrected current density is practically independent of $c_{\text{Na}_2\text{S}_2\text{O}_8}$ if $c_{\text{Na}_2\text{S}_2\text{O}_8} \leq 1 \times 10^{-4}$ M for EP Bi(111) and at $c_{\text{Na}_2\text{S}_2\text{O}_8} \leq 2 \times 10^{-4}$ M for EP Bi(01 $\bar{1}$) electrode (Fig. 18).

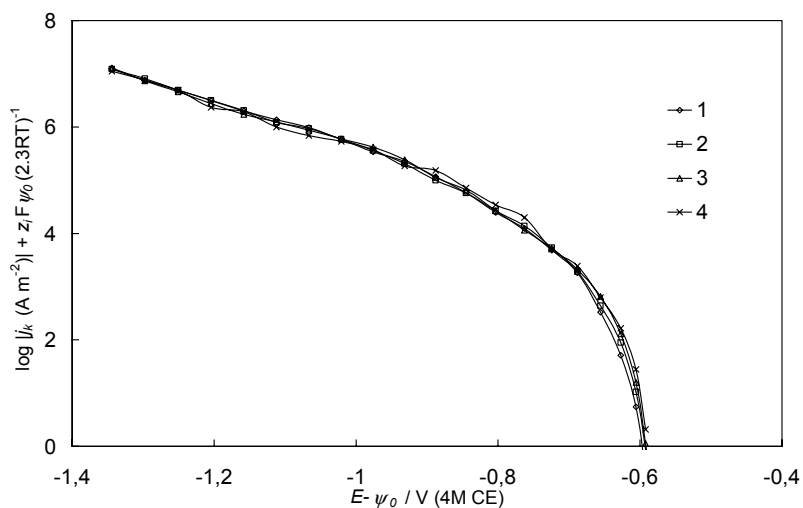


Fig. 18. Corrected Tafel plots ($z_i = -2$ and $\psi_1 = \psi_0$) for EP Bi(01 $\bar{1}$) plane in 0.002M NaF with different additions of Na₂S₂O₈ (M): (1) 2×10^{-5} , (2) 5×10^{-5} , (3) 1×10^{-4} , (4) 2×10^{-4} .

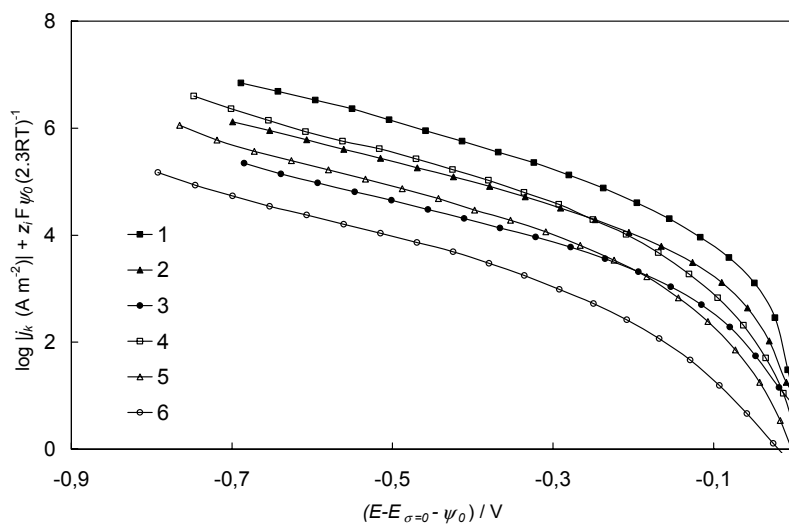


Fig. 19. Corrected Tafel plots ($z_i = -2$ and $\psi_1 = \psi_0$) for EP Bi(01 $\bar{1}$) plane in 1×10^{-4} M Na₂S₂O₈ with additions of x M Na₂SO₄ (1–3) and x M NaF (4–6) with x : (1,4) 0.003, (2,5) 0.007, (3,6) 0.02.

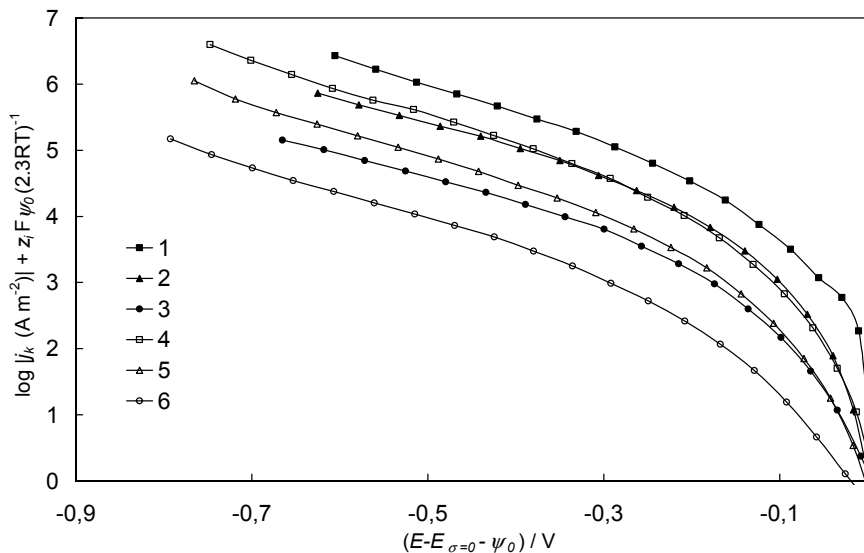


Fig. 20. Corrected Tafel plots ($z_i = -2$ and $\psi_i = \psi_0$) for EP Bi(111) (1–3) and Bi(01 $\bar{1}$) (4–6) in 1×10^{-4} M $\text{Na}_2\text{S}_2\text{O}_8$ with additions of NaF (M): (1,4) 0.003, (2,5) 0.007, (3,6) 0.02.

As it can be seen in Figs. 19 and 20, the corrected kinetic current density values decrease noticeably with increasing $c_{\text{base electrolyte}}$ at fixed $(E - E_{\sigma=0} - \psi_0)$. The corrected Tafel plots for Bi(hkl) electrode are linear at higher negative corrected potentials ($E - E_{\sigma=0} - \psi_0 < -0.4\text{V}$ (4M CE)). However, the slope of the corrected Tafel plots (thus, the transfer coefficient α_{app} obtained from the slope) are slightly lower for Na_2SO_4 base electrolyte compared with NaF base electrolyte solutions (Fig. 21). The slope of the cTp decreases with increasing $c_{\text{base electrolyte}}$ ($\alpha_{\text{app}} = 0.14$ for 0.002M NaF and $\alpha_{\text{app}} = 0.11$ for 0.03M NaF). The same is valid for Bi(01 $\bar{1}$) plane in the case of NaF and Na_2SO_4 ($\alpha_{\text{app}} = 0.12$ for 0.002M and $\alpha_{\text{app}} = 0.11$ for 0.02M Na_2SO_4). The slope values of cTps are practically independent of the concentration of peroxydisulfate anions if $c_{\text{base electrolyte}} = \text{const.}$ and the charge of reactant is taken equal to $z_i = -2$. Experimental data in NaF solutions on Bi(hkl) coincide with the data for Cd(0001) electrode [9–11].

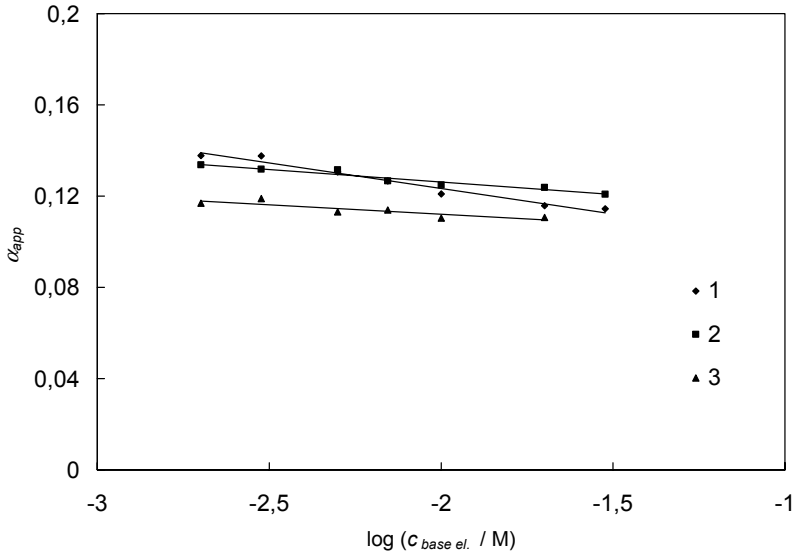


Fig. 21. Apparent transfer coefficient vs. $\log c_{\text{base electrolyte}}$ dependences for EP Bi(111) (1) and Bi(01 $\bar{1}$) (2,3) in the NaF (1,2) and Na₂SO₄ (3) solutions. ($z_i = -2$ and $\psi_1 = \psi_0$)

The cTps for Bi(*hkl*) (Figs. 19 and 20) are nonlinear near the zero charge potential in a good agreement with the Frumkin slow discharge theory [14,17,22,23, 31,43,75] and Gouy-Chapman diffuse layer theory [76–79]. According to these models, the cTps have coincide at $E = E_{\sigma=0}$ as the potential drop in across the diffuse layer vanishes according to the GC model [75–79] as seen in Figs. 19 and 20.

The detailed analysis of cTp shows that the theoretically calculated ψ_1 potential correction caused by the potential drop in the diffuse layer at $\sigma \ll 0$ is very large for the dilute base electrolyte solutions, i.e. the negative values of ψ_0 potential obtained according to GCSG method are very big and thus, the approximation $\psi_1 = \psi_0$ is a very rough one for our systems. Experimentally established less pronounced dependence of cTps on $c_{\text{base electrolyte}}$ is possible to simulate by the variation of two parameters: z_i and ψ_0 potential in cTp equation [9–12,47,61,68,69].

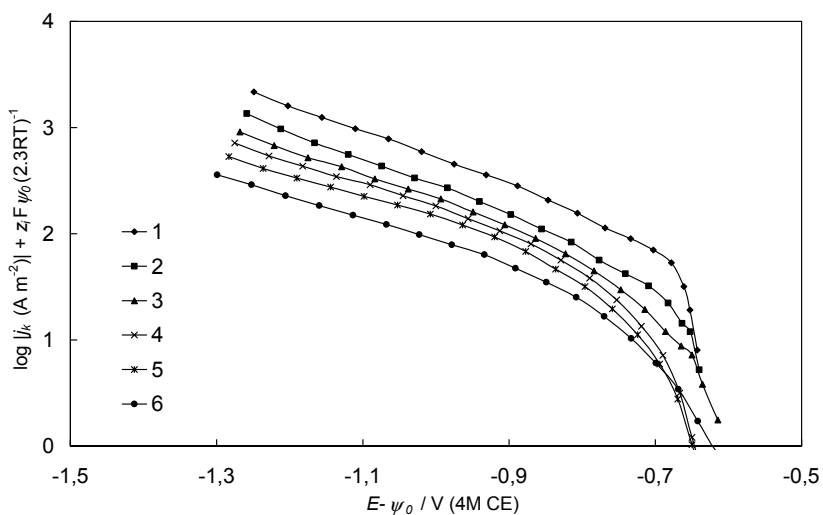


Fig. 22. Corrected Tafel plots at the conditions $z_i = -1$ and $\psi_I = \psi_0$ for EP Bi(111) in 1×10^{-4} M $\text{Na}_2\text{S}_2\text{O}_8$ with additions of NaF (M): (1) 0.002, (2) 0.003, (3) 0.005, (4) 0.007, (5) 0.01, (6) 0.02.

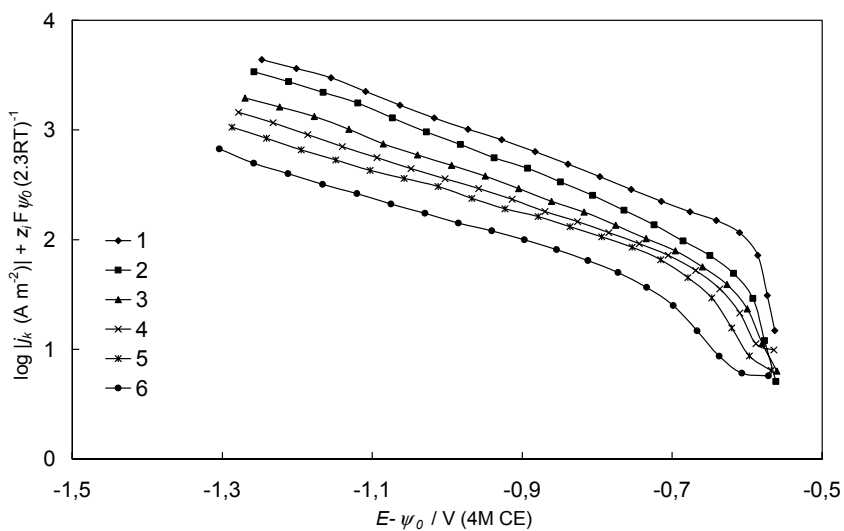


Fig. 23. Corrected Tafel plots at the conditions $z_i = -1$ and $\psi_I = \psi_0$ for EP Bi(011 $\bar{1}$) in 1×10^{-4} M $\text{Na}_2\text{S}_2\text{O}_8$ with additions of Na_2SO_4 (M): (1) 0.002, (2) 0.003, (3) 0.005, (4) 0.007, (5) 0.01, (6) 0.02.

The experimental data in NaF and Na₂SO₄ solutions (Figs. 22 and 23) show that noticeably less pronounced dependence of corrected kinetic current values on the base electrolyte concentration has been established if the ion-pair formation at the outer Helmholtz plane (i.e., in the reaction zone) has been taken into account [9-11,14,17,22,23,31,43,61,68,69]. Thus, it should be noted that the charge transfer mechanism through the adsorbed ion-pairs has been discussed already by Frumkin and co-workers [14,17,23]. If we assume that $z_i = -1$ and $\psi_1 = \psi_0$ then the corrected current density values decrease less with increasing $C_{\text{base electrolyte}}$ at fixed $(E-\psi_0)$ and the values of the transfer coefficient α_{app} are somewhat higher compared with the transfer coefficient calculated at $z_i = -2$. Anyway, the slopes of the cTps are lower for Na₂SO₄ compared with NaF base electrolyte solutions (Fig. 24).

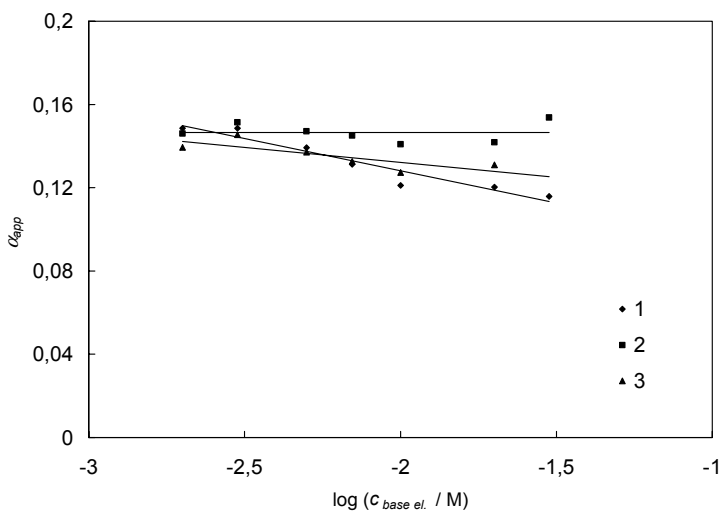


Fig. 24. Apparent transfer coefficient vs. $\log c_{\text{base electrolyte}}$ dependences for EP Bi(111) (1) and Bi(01 $\bar{1}$) (2,3) in the NaF (1,2) and Na₂SO₄ (3) solutions. ($z_i = -1$ and $\psi_1 = \psi_0$)

It should be noted that a good concordance of cTps for EP Bi(111) plane can be established if we assume that the charge number (i.e., the effective charge number of the S₂O₈²⁻ anions) has been calculated using Frumkin- Petrii method [14,17,22,23,31,43]. The results of calculation show (Figs. 25), that the comparatively low absolute values of z_{eff} have been obtained, depending weakly on the chemical nature of the base electrolyte. The decrease in $|z_{eff}|$ at $E \ll E_{\sigma=0}$ in the case of Bi(hkl) indicates the adsorption of cations on the electrode surface which initiated exchange of the reaction mechanism, i.e., the cationic catalysis is possible at $\sigma \ll 0$ [14,17,22-24,31,39,43,59,61,68,69]. Qualitatively the same effect was obtained for Cd(0001)| Na₂S₂O₈ + NaF system too [9-11].

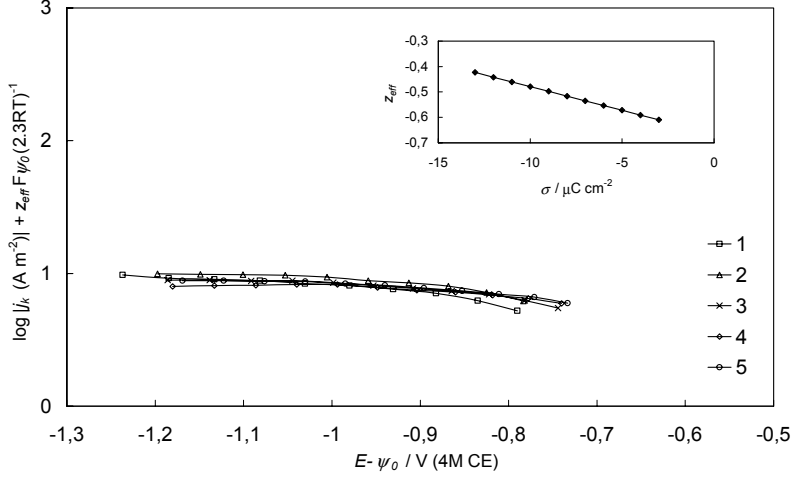


Fig. 25. Corrected Tafel plots calculated at $\psi_l = \psi_0$ and $z_i = z_{eff}$ for EP Bi(111) in 5×10^{-5} M $\text{Na}_2\text{S}_2\text{O}_8$ with additions of NaF (M): (1) 0.003, (2) 0.005, (3) 0.007, (4) 0.01, (5) 0.02.

As mentioned in Ref. [54,64], the ionic association process of the polycharged complex anions (including SO_4^{2-} and $\text{S}_2\text{O}_8^{2-}$ anions) with the base electrolyte cations is possible in the solution phase too. Therefore, the ionic association process in the solution phase has been simulated according to the Fuoss equation [80]

$$K_A = 4\pi N_A a^3 e_0^b / 3000 \quad (9)$$

where $b = e_0^2 / a\epsilon kT$, e_0 is the elementary charge, ϵ is the dielectric constant of the solvent and N_A is the Avogadro number. Comparatively low values of the association constant K_A were obtained ($K_A = 0.118$ for $a = 0.36\text{nm}$) have been calculated according to Eq. (9) assuming that the distance of the closest approach of various ions is fixed at different $a = 0.36; 0.6$ and 0.8 nm, respectively. In these conditions, the kinetic current density is expressed as [11,38,39,51,54]

$$j_k = kc_i \exp\left[\frac{-\alpha(E-\psi_0)F}{RT}\right] \exp\left[\frac{-z_i F\psi_0}{RT}\right] + k_A c_2 \exp\left[\frac{(-z_i+1)(F\psi_0)}{RT}\right] \quad (10)$$

where $z_i = -2$ (charge of the $\text{S}_2\text{O}_8^{2-}$ anion) and $(z_i + 1)$ is the charge of associated $\text{S}_2\text{O}_8^{2-}$ anion with Na^+ (base electrolyte) cation; k_A is the relative rate constant for the reduction reaction of the reactant(s) with $(z_i + 1) = -1$ (NaS_2O_8^-); c_1 and c_2 are the effective volume concentrations of the $\text{S}_2\text{O}_8^{2-}$ anion and NaS_2O_8^- ion, respectively; and k is the rate constant [51]. The results calculated by using Eq. (10) demonstrate a noticeable difference of cTps in the

calculated by using Eq. (10) demonstrate a noticeable difference of cTps in the case of 0.002 and 0.02M NaF as well as Na₂SO₄ base electrolyte solutions (Figs. 26 and 27). Therefore, the ionic association in the solution phase does not have a remarkable influence on the shape and coincidence of cTps for Na₂S₂O₈ + NaF and Na₂S₂O₈ + Na₂SO₄ systems [11,59,68].

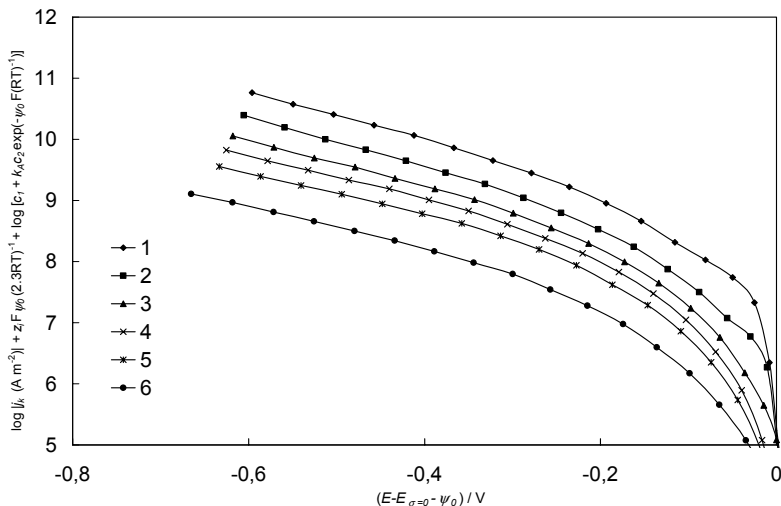


Fig. 26. Corrected Tafel plots calculated according to Eq. (10) at $\psi_1 = \psi_0$ and $z_i = -2$ for EP Bi(111) in 1×10^{-4} M Na₂S₂O₈ with additions of NaF (M): (1) 0.002, (2) 0.003, (3) 0.005, (4) 0.007, (5) 0.01, (6) 0.02.

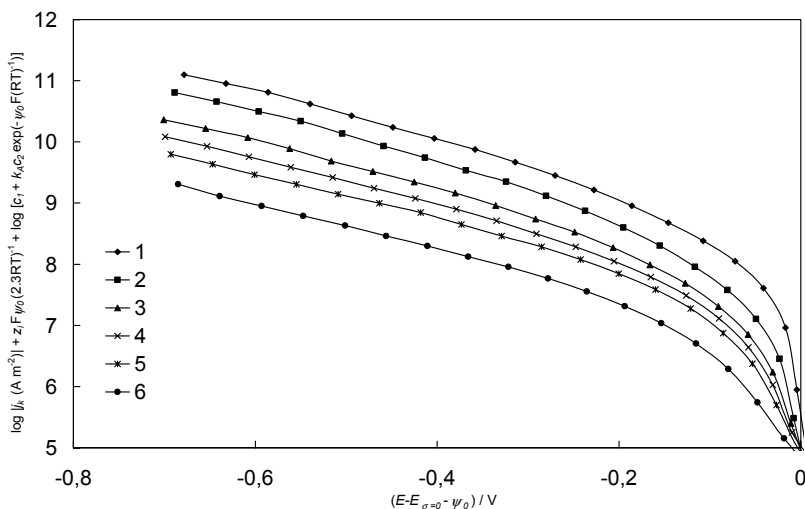


Fig. 27. Corrected Tafel plots calculated according to Eq. (10) at $\psi_1 = \psi_0$ and $z_i = -2$ for EP Bi(011̄) in 1×10^{-4} M Na₂S₂O₈ with additions of Na₂SO₄ (M): (1) 0.002, (2) 0.003, (3) 0.005, (4) 0.007, (5) 0.01, (6) 0.02.

According to the results of classical works [14,17,22,53,55], the linear corrected Tafel plots for $\text{Hg} | \text{S}_2\text{O}_8^{2-}$ system were obtained if it was assumed that the reaction site lies in the inner layer (i.e., $(x_i - x_d) < 0$), but surprisingly for $\text{Hg} | [\text{Fe}(\text{CN})_6]^{3-}$ system the reaction site has to lie in the diffuse layer ($(x_i - x_d) > 0$). The results of simulation of the data for the $\text{Bi}(hkl)$ in $\text{Na}_2\text{S}_2\text{O}_8 + \text{NaF}$ or Na_2SO_4 aqueous solutions show that in spite of the selected fixed values of $(x_i - x_d) > 0$ (0; 0.20; 0.43; 0.68 nm) in Eq. (3) the cTps obtained are nonlinear and there is no concordance for cTps measured in a wide concentration region of the base electrolyte (Figs. 28 and 29). The values of apparent transfer coefficient are comparatively low especially for $\text{Na}_2\text{S}_2\text{O}_8 + \text{Na}_2\text{SO}_4$ system and depending weakly on the concentration of the base electrolyte in the solution (Fig. 30).

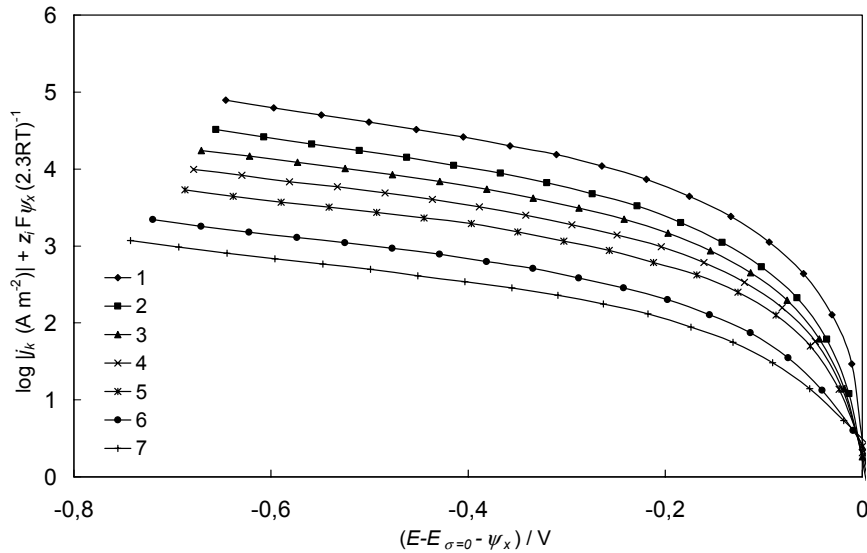


Fig. 28. Corrected Tafel plots calculated according to Eq. (3) ($\psi_l = \psi_x$ and $z_i = -2$) for EP Bi(111) in 5×10^{-5} M $\text{Na}_2\text{S}_2\text{O}_8$ with additions of NaF (M): (1) 0.002, (2) 0.003, (3) 0.005, (4) 0.007, (5) 0.01, (6) 0.02, (7) 0.03 at the fixed distance of reaction site from the outer Helmholtz plane $(x_i - x_d) = 0.43$ nm.

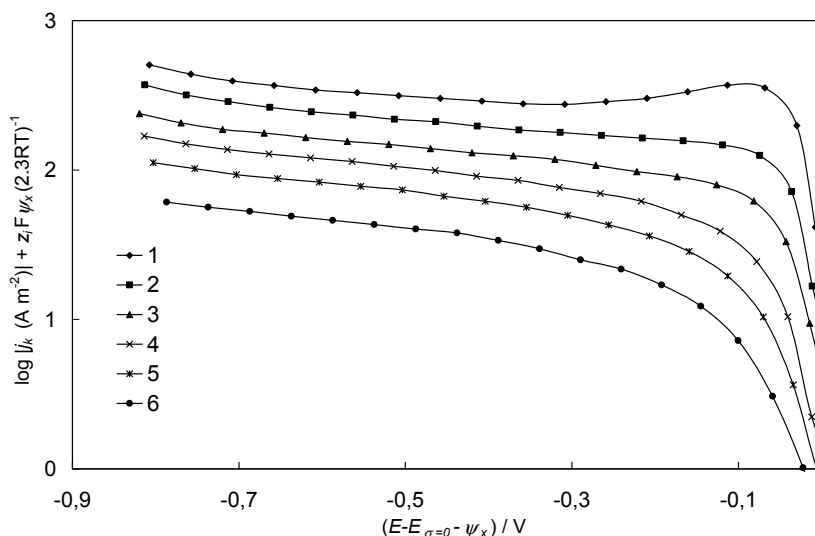


Fig. 29. Corrected Tafel plots calculated according to Eq. (3) at $\psi_l = \psi_x$ and $z_i = -2$ for EP Bi(01 $\bar{1}$) in 5×10^{-5} M $\text{Na}_2\text{S}_2\text{O}_8$ with additions of Na_2SO_4 (M): (1) 0.002, (2) 0.003, (3) 0.005, (4) 0.007, (5) 0.01, (6) 0.02 at the fixed distance of reaction site from the outer Helmholtz plane ($x_l - x_d$) = 0.43 nm.

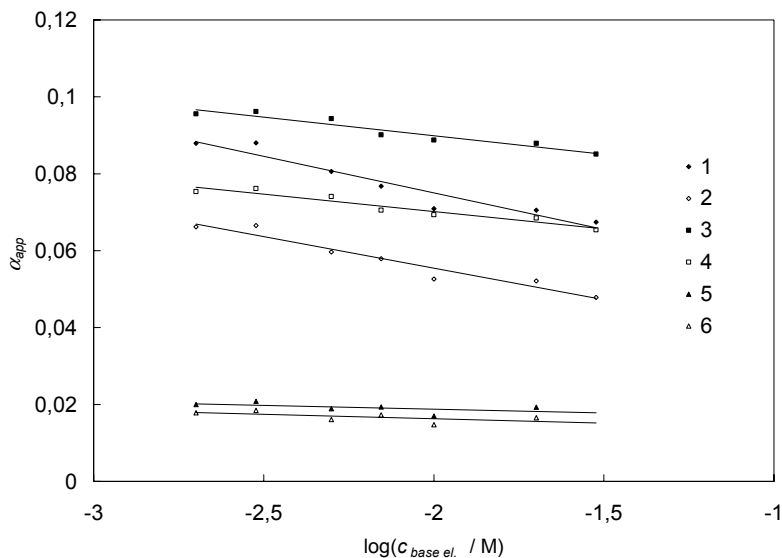


Fig. 30. Apparent transfer coefficient vs. $\log c_{\text{base electrolyte}}$ dependences for EP Bi(111) (1,2) and Bi(01 $\bar{1}$) (3–6) in the NaF (1–4) and Na_2SO_4 (5,6) solutions. ($z_i = -2$ and $\psi_l = \psi_x$) and ψ_x calculated according to Eq. (3) at the fixed distances of reaction site from the outer Helmholtz plane ($x_l - x_d$) (nm): (1,3,5) 0.20, (2,4,6) 0.43.

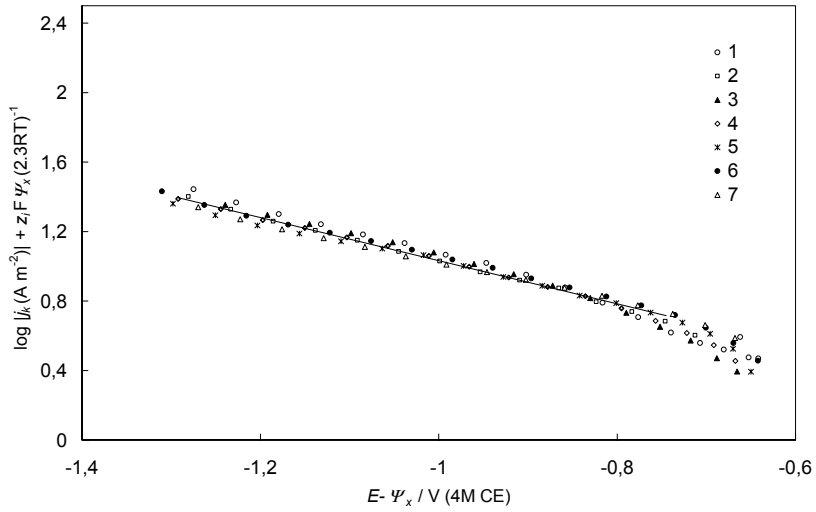


Fig. 31. Corrected Tafel plots calculated according to Eq. (3) at $\psi_l = \psi_x$ and $z_i = -0.58$ for EP Bi(111) in 5×10^{-5} M $\text{Na}_2\text{S}_2\text{O}_8$ with additions of NaF (M): (1) 0.002, (2) 0.003, (3) 0.005, (4) 0.007, (5) 0.01, (6) 0.02, (7) 0.03; assuming that $(x_i - x_d) = f(c_{\text{NaF}})$ and the term $[-\kappa(x_i - x_d)] = \text{const.}$

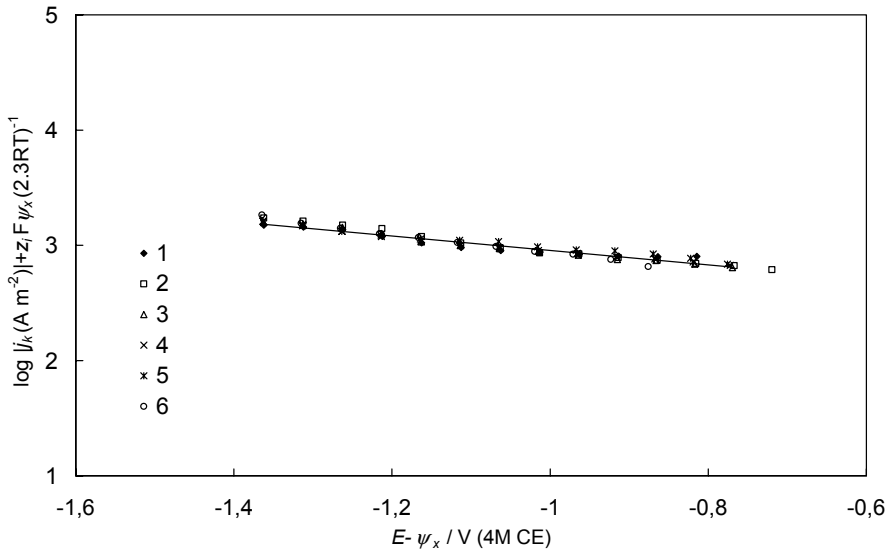


Fig. 32. Corrected Tafel plots calculated according to Eq. (3) at $\psi_l = \psi_x$ and $z_i = -2$ for EP Bi(011) in 1×10^{-4} M $\text{Na}_2\text{S}_2\text{O}_8$ with additions of Na_2SO_4 (M): (1) 0.002, (2) 0.003, (3) 0.005, (4) 0.007, (5) 0.01, (6) 0.02; assuming that $(x_i - x_d) = f(c_{\text{Na}_2\text{SO}_4})$ and the term $[-\kappa(x_i - x_d)] = \text{const.}$

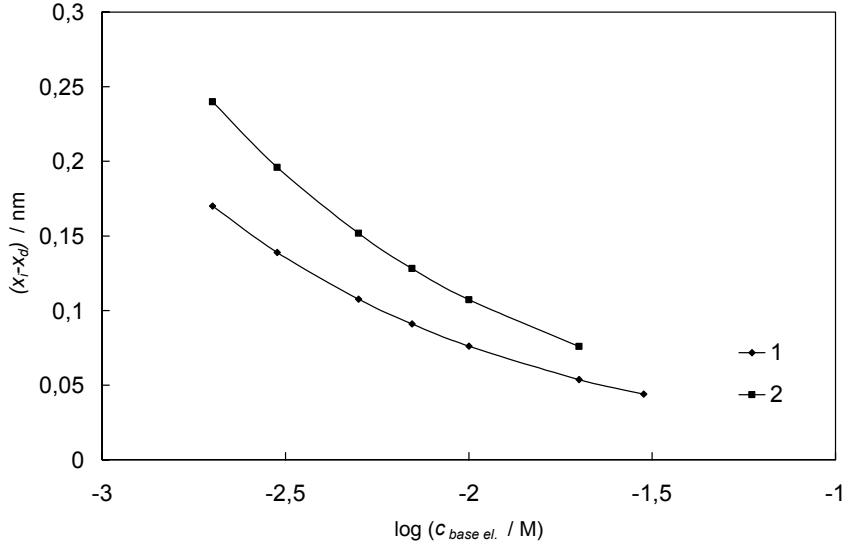


Fig. 33. The dependences of the effective distance of the reaction site from the outer Helmholtz plane on the base electrolyte concentration for EP Bi(111) in the NaF (1) and Bi(01 $\bar{1}$) in the Na₂SO₄ (2) solutions using Eq.(3) and data in Figs. 31 and 32.

Analysis of the experimental cTps shows that the coincidence and linearity of the cTps (Figs. 31 and 32) at $E-\psi_x$ can be obtained if we assume that the distance of the closest approach of the reacting anions to the electrode surface ($x_i - x_d$) depends on the base electrolyte concentration (i.e. $(x_i - x_d) = f(c_{\text{base electrolyte}})$) (Fig. 33) and the concordance of cTps can be reached if the term in the last brackets of Eq. (3) $[-\kappa(x_i - x_d)] \approx \text{const.}$ at $E = \text{const.}$ Thus, if we assume that the diffuse layer theory is correct and the Gouy length κ can be calculated by Eq. (4) [22,23,71,77–79] and the value of the ψ_x potential at the reaction site can be calculated by Eq. (3) then it is possible to calculate the effective distance values of the reaction site from the outer Helmholtz plane ($x_i - x_d$) = $f(c_{\text{base electrolyte}})$, assuming that the corrected Tafel plots have to be linear and coincide for different $c_{\text{base electrolyte}}$. The results in Figs. 31 and 32 show that this is valid if we assume that $(x_i - x_d)$ is an exponential function of the base electrolyte concentration. Thus, if this effect has a real physical background then we can conclude that the effective distance of the reaction site from the Bi(hkl) surface (as well as from the outer Helmholtz plane) increases exponentially with diluting the electrolyte solution, i.e., with increasing the effective ion atmosphere thickness according to the Debye-Hückel theory. According to Fig. 33, a better fit of the experimental data has been established in the case of comparatively small $(x_i - x_d)$ values for more concentrated base electrolyte solution and, thus, the reaction site lies not far from the outer

Helmholtz plane for the Bi(*hkl*) electrodes. The weak dependence of the effective distance of the reaction site on the chemical nature of the base electrolyte anion can be explained by the different so-called “squeezing out” effects [14,17,22,23,60,64–66,68–71,76,81–84], i.e., by the dependence of the distance of the closest approach of the reacting ions to the electrode surface on the base electrolyte concentration and geometrical structure of the F⁻ or SO₄²⁻ anion. The values of ($x_i - x_d$) are somewhat higher for Bi(*hkl*) electrode compared with Cd(0001) single crystal plane [9–11]. This effect can be explained by lower water adsorption energy [9–11,56–61,64–66,68,69,71,81–83] for Bi(*hkl*) plane and, thus, by less compact inner layer structure in comparison with Cd(0001) electrode (i.e., by the smaller distances of the closest approach of the S₂O₈²⁻ anion to the Cd(0001) plane). It should be noted that the potential drop in the thin metal surface layer is higher for the more semimetallic Bi(*hkl*) than that for Cd(0001) plane [9–11,56–66,68,69,81–83] and thus the “spill over” of the “free” electrons from Bi(*hkl*) is more pronounced than that for Cd(0001) plane.

It should be noted that there are deviations from the classical Gouy-Chapman-Grahame model for Bi(*hkl*) electrode in NaF and Na₂SO₄ solutions with different concentration [56,60,62–66,70,71,81–84], i.e., the inner layer capacitance depends on the electrolyte concentration. The electrical double layer (i.e. ψ_0 potential) correction for the systems with the weak specific adsorption of anions is a very complicated problem even for systems with the constant ionic strength where no electrochemical reaction occurs [56,58,59,62–66]. The systematic analysis of experimental data for Bi(*hkl*) [65,71] shows that the ψ_0 potential values calculated using classical Gouy-Chapman-Grahame model [76–79] are overestimated (i.e. the negative values of ψ_0 potential are too large to give the linear and coincided corrected Tafel plots at $\sigma < 0$). The situation is more complicated for the systems with smaller ionic strength. Thus, it can be concluded that the classical $|\psi_0|$ potential corrections are too high to give the concordance for the cTps at surface charge densities $\sigma \ll 0$ within the wide base electrolyte concentration region studied. This conclusion is in good agreement with the results for [Co(NH₃)₆]³⁺ and [Fe(CN)₆]³⁻ electroreduction on Bi(*hkl*) and Cd(0001) electrodes [12,47].

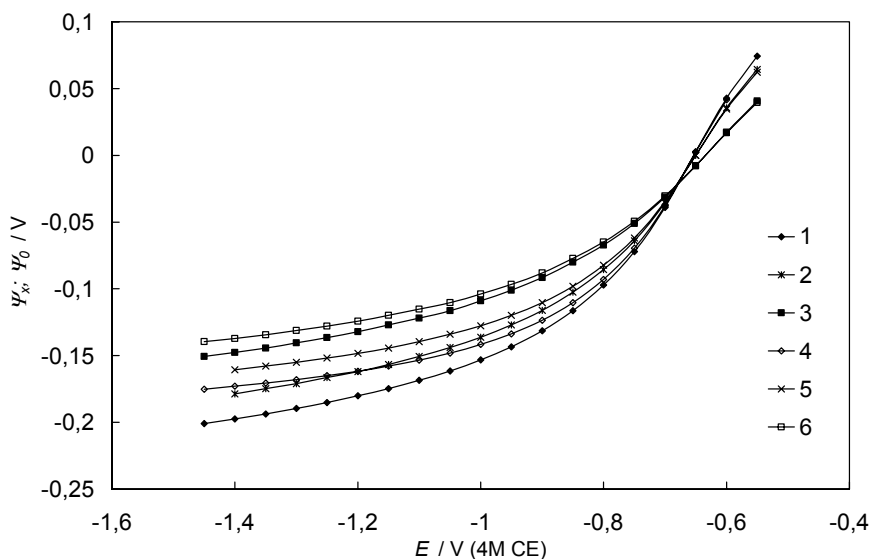


Fig. 34. Classical Gouy-Chapman ψ_0 potential (1–3) and effective ψ_x potential (4–6) (used for the calculation of cTps in Fig. 31) vs electrode potential dependences for EP Bi(111) electrode in NaF solution (M): (1,4) 0.002, (2,5) 0.005, (3,6) 0.02; assuming that $(x_r-x_d)=f(c_{NaF})$ and the term $[-\kappa(x_i-x_d)]=const.$

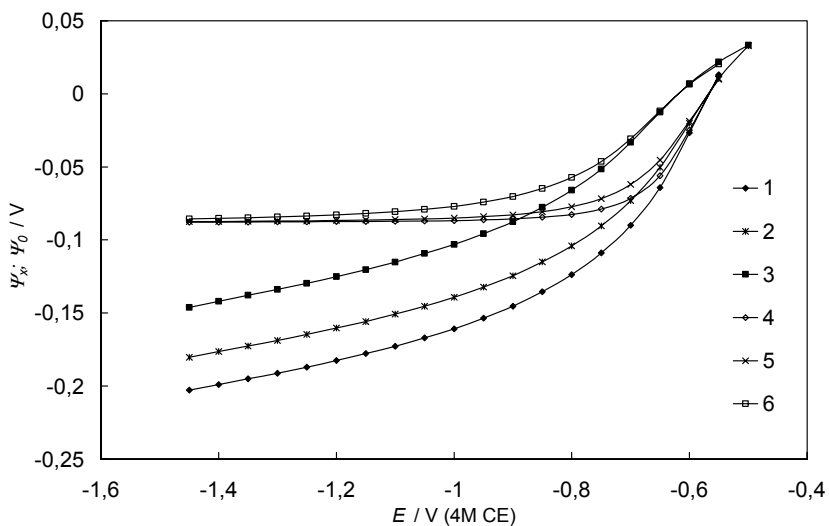


Fig. 35. Classical Gouy-Chapman ψ_0 potential (1–3) and effective ψ_x potential (4–6) (used for the calculation of cTps in Fig. 32) vs electrode potential dependences for EP Bi(01 $\bar{1}$) electrode in Na₂SO₄ solution (M): (1,4) 0.002, (2,5) 0.005, (3,6) 0.02; assuming that $(x_r-x_d)=f(c_{Na_2SO_4})$ and the term $[-\kappa(x_i-x_d)]=const.$

The ψ_x potential values were calculated according to Eq. (3) assuming that $(x_i - x_d) = f(c_{\text{base electrolyte}})$ and $[-\kappa(x_i - x_d)] \approx \text{const.}$ at $E = \text{const.}$ Comparison of the ψ_0 potential values with the ψ_x potential values (Figs. 34 and 35) shows that the values of $|\psi_x|$ are lower than $|\psi_0|$ and at very high negative surface charge densities ($E < -1.4\text{V}$ vs 4M CE) there is only a weak dependence of ψ_x potential on $c_{\text{base electrolyte}}$ in Na_2SO_4 solutions. Thus, at comparatively negative surface charge densities the influence of diffuse layer (i.e. the base electrolyte concentration) on the charge transfer kinetics is very small caused probably by the charge transfer through the adsorbed ion-pairs [8,14,17,30,32,43,59,61, 68,69].

The data in Fig. 36 show that the values of transfer coefficient α_{app} , obtained from cTps in Figs. 31 and 32, are practically independent of the base electrolyte concentration on $\text{Bi}(01\bar{1})$ plane and values of α_{app} for NaF are higher than for Na_2SO_4 base electrolyte. The very low values of α_{app} for systems $\text{Na}_2\text{S}_2\text{O}_8 + \text{base electrolyte}$ on $\text{Bi}(hkl)$ electrode indicate that the activationless electroreduction process is possible at high negative surface charge densities (at $E \ll E_{\sigma=0}$) as well as at $\text{Cd}(0001) | \text{base electrolyte} + \text{Na}_2\text{S}_2\text{O}_8$ interface [9–11], which is in good agreement with the Levich model [30,32] and quantum chemical calculation data for the Hg electrode [38,39].

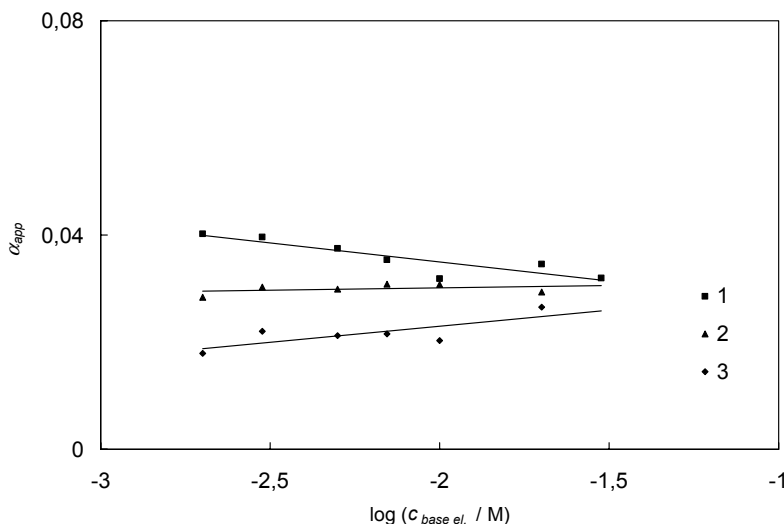


Fig. 36. Apparent transfer coefficient vs. $\log c_{\text{base electrolyte}}$ dependences for EP Bi(111) in the NaF (1) and Bi(01 $\bar{1}$) in the NaF (2) and in the Na_2SO_4 (3) solutions, assuming that $(x_i - x_d) = f(c_{\text{base electrolyte}})$ and the term $[-\kappa(x_i - x_d)] = \text{const.}$ in Eq.(3).

Fawcett et al. [85–87] developed a model for the diffuse layer potential correction based on the generalised field spherical approximation (GFSA), but the corrections obtained for NaF and Na_2SO_4 base electrolyte solutions for Bi(hkl) and Cd(0001) electrode using Fawcett et al. model only weakly differ

from those obtained according to the GCSG model as the comparatively dilute base electrolyte solutions ($c_{\text{base electrolyte}} \leq 0.02$ M) have been used in our studies. According to the Gonzalez-Sanz model for the diffuse layer [44] and Damaskin et al. analysis [8], the activity of the electrolyte instead of concentration should be used as the so-called concentration variable. These corrections are small for the NaF 1:1 electrolyte solutions but in case of Na_2SO_4 1:2 electrolyte solutions the linear C_{exp}^{-1} , C_D^{-1} plots (i.e., the experimental capacitance vs. calculated diffuse layer capacitance according to the Gonzalez-Sanz theory plots) have been established (Fig 37) only if the Gonzalez-Sanz model [44] has been used. The values of the inner layer capacitance C_H in the case of Na_2SO_4 are in good agreement with those for NaF.

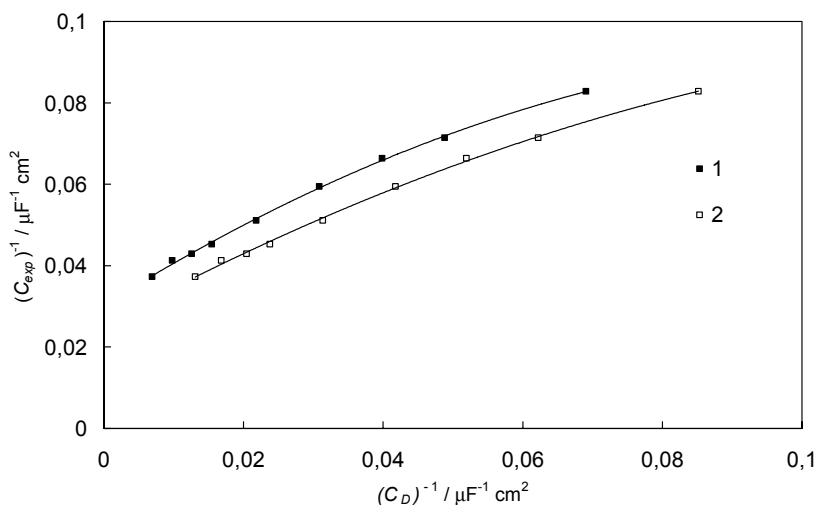


Fig. 37. Dependences of the inverse experimental differential capacitance on the calculated inverse diffuse layer capacitance according to the Gouy-Chapman (1) and Gonzalez-Sanz (2) models for the EP Bi(011) electrode in the base electrolyte (Na_2SO_4) solution.

The dependences of the kinetic current density, corrected for the medium activity coefficient according to [18,44], on the electrical variable ($E-E_{\sigma=0}-\psi_0$) are given in Figs. 38 and 39.

The current density values have been corrected according to Eq. (11)

$$\log\left(j_k \frac{c_i}{c_i^{(2)}}\right) \approx \log j_k - \log(1 - f_0^\infty) \quad (11)$$

where $c_i^{(2)}$ is the concentration of $S_2O_8^{2-}$ anions at the outer Helmholtz plane and f_0^∞ is the activity coefficient of $S_2O_8^{2-}$ in the bulk of solution.

As shown in Figs. 38 and 39, noticeably less pronounced dependence of corrected current density on $c_{\text{base electrolyte}}$ has been established in comparison with the cTps obtained using classical Frumkin correction [14,17,22,23,31,37, 43,59,61,68,69]. However, the cTps are nonlinear near zero charge potential for all system studied. According to the experimental data there is a very small dependences of cTps on the concentration of peroxodisulfate anions and there is no big difference between cTps calculated for EP Bi(111) and Bi(01 $\bar{1}$) planes. However, according to calculations made for CHE Bi(111) there are big deviations of cTp from the data for EP Bi(111) plane indicating that the nanoscopic surface structure (Figs. 1–3) of electrode surface has very big influence on the inner layer structure as well as on the diffuse layer correction i.e. on the microscopic $\psi_s(x_i)$ values.

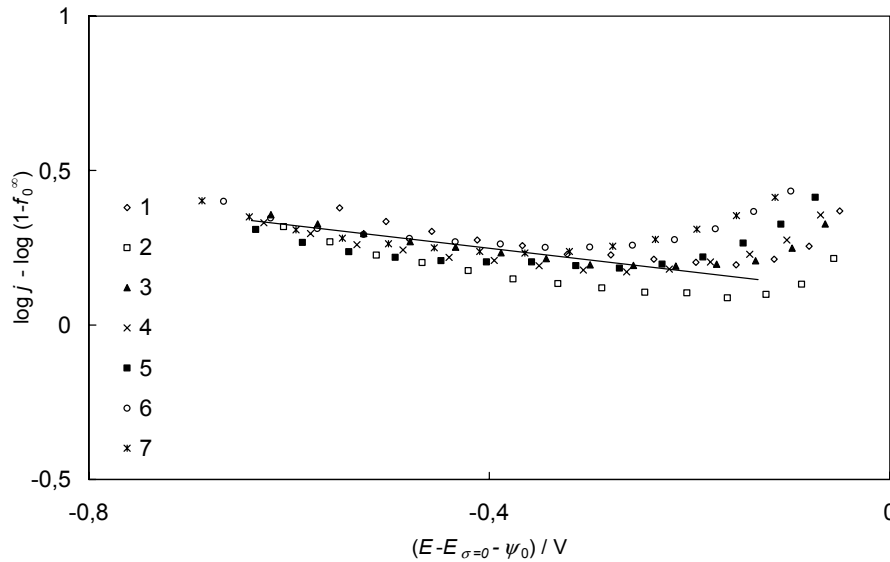


Fig. 38. The $\log j_k - \log(1 - f_0^\infty)$ dependences (calculated according to Gonzalez-Sanz [44] and Damaskin et al. [8] models) for EP Bi(111) in 5×10^{-5} M $Na_2S_2O_8$ with additions of NaF (M): (1) 0.002, (2) 0.003, (3) 0.005, (4) 0.007, (5) 0.01, (6) 0.02, (7) 0.03.

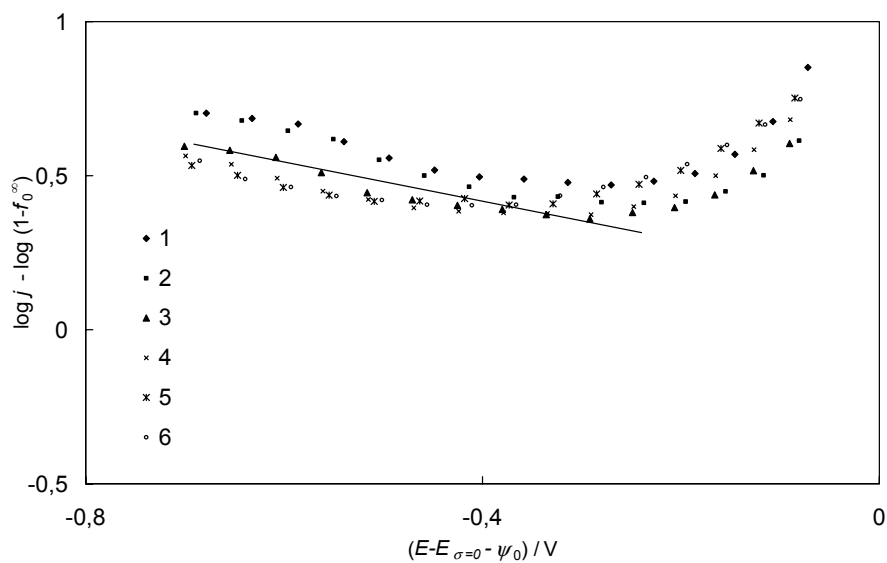


Fig. 39. The $\log j_k - \log(1 - f_0^\infty)$ dependences (calculated according to Gonzalez-Sanz [44] and Damaskin et al. [8] models) for EP Bi(011̄) in 1×10^{-4} M $\text{Na}_2\text{S}_2\text{O}_8$ with additions of Na_2SO_4 (M): (1) 0.002, (2) 0.003, (3) 0.005, (4) 0.007, (5) 0.01, (6) 0.02.

7. CONCLUSIONS

The electroreduction kinetics of peroxodisulfate anion at electrochemically polished Bi(111) and Bi(01 $\bar{1}$) planes has been studied by cyclic and rotating disc electrode voltammetry methods. It was found that the rate of electroreduction of $S_2O_8^{2-}$ anion depends on the potentials of Bi electrode, on the concentration of $S_2O_8^{2-}$ anions, as well as on the concentration of base electrolyte solution and on the nature of base electrolyte anions. In experiments NaF and Na_2SO_4 as base electrolytes, were used. It was found that there is a dependence of the kinetic parameters on the electrode surface pre-treatment method used. In the region of zero charge potential the electroreduction of $S_2O_8^{2-}$ anion is mainly limited by the rate of diffusion step of $S_2O_8^{2-}$ anions. In the region of small negative surface charge densities the inhibition of $S_2O_8^{2-}$ anion electroreduction takes place.

The apparent rate constant k_{het} values have been calculated using kinetic current densities j_k and the $\log k_{het}$ values at $E < E_{\sigma=0}$ weakly rise with base electrolyte concentration.

The different models for the calculation of the diffuse layer potential correction on the kinetic current density have been used to construct the so-called corrected Tafel plots. Analysis of the corrected Tafel plots for solutions with different base electrolyte concentrations shows that the concordance of cTps has been established if it was assumed that the effective distance of the reaction site from the outer Helmholtz plane depends inversely on the base electrolyte concentration in the mixed electrolyte solution. The values of apparent transfer coefficient α_{app} , corrected for the double layer effect, noticeably lower than 0.5 for the Bi(hkl) planes. α_{app} only very weakly depends on the electrolyte concentration, have been obtained. The very low values of the apparent charge transfer coefficient show that the activationless charge transfer mechanism is possible for base electrolyte + $Na_2S_2O_8$ systems on Bi(hkl) planes. This conclusion is in a good agreement with the theoretical model calculations for the high hydrogen overvoltage metals (mainly for the Hg electrode) based on the diabatic charge transfer mechanism from the metal to an ion. The corrected Tafel plots for chemically etched Bi(hkl) have very complicated shape and it is impossible to use these data for the detailed quantitative analysis of the reaction mechanism at polycrystalline solid surface|electrolyte interface.

8. REFERENCES

- [1] A.Hamelin, M.J. Weaver, *J. Electroanal. Chem.* 209 (1986) 109.
- [2] M. Hromadova, W.R. Fawcett, *J. Phys. Chem.* 104 (2000) 4356.
- [3] Z. Samec, K. Doblhofer, *J. Electroanal. Chem.* 367 (1994) 141.
- [4] Z. Samec, K. Doblhofer, *J. Electroanal. Chem.* 409 (1996) 165.
- [5] Z. Samec, K. Doblhofer, *J. Electroanal. Chem.* 432 (1997) 205.
- [6] Z. Samec, K. Kirscher, K. Doblhofer, *J. Electroanal. Chem.* 499 (2001) 129.
- [7] R.R. Nazmutdinov, G.A. Tsirlina, Yu.I. Kharkats, O.A. Petrii and M. Probst, *J. Phys. Chem.* 52 (1998) 677.
- [8] B.B. Damaskin, E.V. Stenina, O.A. Baturina and L.N. Sviridova, *Elektrokhimiya* 34 (1998) 1083.
- [9] T. Thomborg, E. Lust, *J. Electroanal. Chem.* 485 (2000) 89.
- [10] T. Thomborg, J. Nerut, K. Lust, E. Lust, *Electrochim. Acta* 49 (2004) 1271.
- [11] T. Thomborg, J. Nerut, R. Jäger, P. Möller, K. Lust, E. Lust, *J. Electroanal. Chem.* 586 (2006) 237.
- [12] R. Jäger, E. Härk, P. Möller, J. Nerut, K. Lust, E. Lust, *J. Electroanal. Chem.* 566 (2004) 217.
- [13] A.N. Frumkin, *Z. Phys. Chem.* 164 (1953) 121.
- [14] A.N. Frumkin, *Z. Elektrochem.* 59 (1955) 807.
- [15] A.N. Frumkin, in: P. Delahay (Ed.), *Advances in Electrochemistry*, vol. 1, Interscience Publ., New York, 1961 p. 65.
- [16] R. Parsons, *Surf. Sci.* 2 (1964) 418.
- [17] A.N. Frumkin, N.V. Nikolayeva-Fedorovich, N.P. Berezina, H.E. Keis, *J. Electroanal. Chem.* 58 (1975) 189.
- [18] W.R. Fawcett, in: J. Lipkowski, P.N. Ross (Eds.), *Electrocatalysis*, Wiley, New York, 1998, p. 323 (Chapter 8).
- [19] W.R. Fawcett, M. Hromadova, G.A. Tsirlina, R.R. Nazmutdinov, *J. Electroanal. Chem.* 498 (2001) 93.
- [20] M.J. Weaver, F.C. Anson, *J. Am. Chem. Soc.* 97 (1975) 4403.
- [21] A. Hamelin, M.J. Weaver, *J. Electroanal. Chem.* 223 (1987) 171.
- [22] A.N. Frumkin, *Potentsialy nulevogo zaryada*, Nauka, Moscow, 1982, p. 227-258.
- [23] A.N. Frumkin, *Elektrodnye protsessy*, Nauka, Moscow, 1987.
- [24] A.N. Frumkin and G.M. Florianovich, *Dokl. Akad. Nauk SSSR* 80 (1951) 907.
- [25] G.M. Florianovich and A.N. Frumkin, *Zh.Fiz.Khim.* 29 (1955) 1827.
- [26] N.V. Fedorovich, A.N. Frumkin and H.E. Keis, *Coll.-Czech. Chem Comm.* 36 (1971) 722.
- [27] N.V. Nikolaeva-Fedorovich, M.D. Levi and S.I. Kulakovskya, *Elektrokhimiya* 13 (1977) 904.
- [28] N.V. Fedorovich and F.S. Sarbash, *Dokl. Akad. Nauk SSSR* 255 (1980) 923.
- [29] M.D. Levi, N.V. Fedorovich and B.B. Damaskin, *Can. J. Chem.* 59 (1981) 2019.
- [30] V.G. Levich, *Fiziko-khimicheskaya gidrodinamika*, Fizmatgiz, Moscow, 1959, p.161.
- [31] A.N. Frumkin, O.A. Petrii, *Dokl. Akad. Nauk SSSR* 147 (1962) 418.
- [32] V.G. Levich, *Dokl. Akad. Nauk SSSR* 124 (1959) 869.
- [33] L.Gierst, in E. Yeager (Ed.), *Trans. of the Symp. on Electrode Processes*, Wiley, New York, 1961, p. 109.

- [34] W. Fawcett, S. Levie, *J. Electroanal. Chem.* 43 (1973) 301.
- [35] W. Fawcett, D. Bieman and M. Mackey, *Coll.-Czech. Chem Comm.* 36 (1971) 503.
- [36] W. Fawcett, *J. Electroanal. Chem.* 22 (1969) 19.
- [37] P. Delahay and A. Aramata, *J. Phys. Chem.* 66 (1962) 1194.
- [38] R.R. Nazmutdinov, D.V. Gluhov, G.A. Tsirlina, O.A. Petrii, *Elektrokhimiya* 38 (2002) 812.
- [39] R.R. Nazmutdinov, D.V. Gluhov, O.A. Petrii, G.A. Tsirlina, G.N. Botikova, *J. Electroanal. Chem.* 552 (2003) 261.
- [40] J.-M. Saveant, *J. Am. Chem. Soc.* 114 (1992) 10595.
- [41] D.M. Stanbury, in: A.G. Sykes (Ed.), *Adv. Inorg. Chem.* 33 (1989) 69.
- [42] J. Song, H. Fu, W. Guo, *J. Electroanal. Chem.* 511 (2001) 31.
- [43] O.A. Petrii, A.N. Frumkin, *Dokl. Akad. Nauk SSSR* 146 (1962) 1121.
- [44] R. Gonzalez, F. Sanz, *Electroanalysis* 9 (1997) 169.
- [45] P. Delahay, *Double Layer and Electrochemical Kinetics*, Interscience, New York, 1965.
- [46] R.R. Nazmutdinov, D.V. Gluhov, G.A. Tsirlina, O.A. Petrii, *Elektrokhimiya* 39 (2003) 105.
- [47] J. Nerut, P. Möller, E. Lust, *Electrochim. Acta* 49 (2004) 1597.
- [48] G.A. Tsirlina, Y.I. Kharkats, R.R. Nazmutdinov, O.A. Petrii, *Russ. J. Electrochem.* 35 (1999) 23.
- [49] G.A. Tsirlina, O.A. Petrii, Y.I. Kharkats, A.M. Kuznetsov, *Russ. J. Electrochem.* 35 (1999) 1372.
- [50] R.R. Nazmutdinov, I.V. Pobelov, G.A. Tsirlina, O.A. Petrii, *J. Electroanal. Chem.* 491 (2000) 126.
- [51] G.A. Tsirlina, N.V. Titova, R.R. Nazmutdinov, O.A. Petrii, *Russ. J. Electrochem.* 37 (2001) 21.
- [52] R.R. Nazmutdinov, G.A. Tsirlina, Y.I. Kharkats, O.A. Petrii, A.M. Kuznetsov, *Electrochim. Acta* 45 (2000) 3521.
- [53] O.A. Petrii, N.V. Nikolayeva-Fedorovich, *J. Fhiz. Khim.* 35 (1961) 1999.
- [54] G.A. Tsirlina, O.A. Petrii, R.R. Nazmutdinov, D.V. Gluhov, *Russ. J. Electrochem.* 38 (2002) 154.
- [55] A.N. Frumkin, O.A. Petrii, N.V. Nikolayeva-Fedorovich, *Dokl. Akad. Nauk SSSR* 128 (1959) 1006.
- [56] E. Lust, K. Lust, A. Jänes, *Russ. J. Electrochem.* 31 (1995) 807.
- [57] S. Kallip, E. Lust, *Electrochem. Comm.* 7 (2005) 863.
- [58] K.K. Lust, E.J. Lust, M.A. Salve, U.V. Palm, *Elektrokhimiya* 25 (1989) 1578.
- [59] E. Lust, J. Nerut, E. Härk, S. Kallip, V. Grozovski, T. Thomberg, R. Jäger, K. Lust, K. Tähnas, *ECS Transactions*, 1 (17) (2006) 9.
- [60] E. Lust, A. Jänes, K. Lust, M. Väärtnõu, *Electrochim. Acta* 42 (1997) 771.
- [61] E. Lust, R. Truu, K. Lust, *Russ Electrochem.* 36 (2000) 1195.
- [62] B. Damaskin, U. Palm, M. Väärtnõu, *J. Electroanal. Chem.* 70 (1976) 103.
- [63] U.V. Palm, B.B. Damaskin, *Itogi Nauki I Tekhniki*, vol. 12, VINITI, Moscow, 1977, p. 99.
- [64] K. Lust, M. Väärtnõu, E. Lust, *Electrochim. Acta* 45 (2000) 3543.
- [65] K. Lust, E. Lust, *J. Electroanal. Chem.* 552 (2003) 129.
- [66] R.R. Nazmutdinov, T.T. Zinkicheva, M. Probst, K. Lust, E. Lust, *Surf. Sci.* 577 (2005) 112.

- [67] J. Desilvestro and M.J. Weaver, *J. Electroanal. Chem.* 234 (1987) 237.
- [68] R. Jäger, K. Lust, S. Kallip, V. Grozovski, E. Lust, Influence of surface nano-roughness of Bi electrodes on the electroreduction kinetics of $S_2O_8^{2-}$ anion, *J. Solid State Electrochem* (in press)
- [69] T. Thomberg, R. Jäger, E. Lust, Impedance spectroscopy data for $S_2O_8^{2-}$ anions electroreduction at Bi(111) plane, *J. Electroanal. Chem* (in press).
- [70] E. Lust, K. Lust, A. Jänes, *J. Electroanal. Chem.* 413 (1996) 111.
- [71] S. Trasatti, E. Lust, in: R.E. White, B.E. Conway, J.O'M. Bockris (Eds.), *Modern Aspects of Electrochemistry*, vol. 33, Kluwer Academic/Plenum Publishers, New York and London, 1999, p. 1.
- [72] K. Lust, E. Perkson, E. Lust, *J. Russ. Electrochem.* 36 (2000) 1257.
- [73] A.N. Frumkin, E.A. Aikazyan, *Dokl. Akad. Nauk SSSR* 100 (1955) 315.
- [74] A.N. Frumkin, E. Tedoradze, *Z. Elektrochem.* 62 (1958) 252.
- [75] L.I. Krishtalik, *Elektrokhimiya* 6 (1970) 507.
- [76] W. Schmickler, *Interfacial Electrochemistry*, Oxford University Press, New York, Oxford, 1996.
- [77] G. Gouy, *J. Phys. Radium* 9 (1910) 457.
- [78] D. Chapman, *Philos. Mag.* 25 (1913) 475.
- [79] D.C. Grahame, *Chem. Rev.* 41 (1947) 441.
- [80] R.M. Fuoss, *J. Am. Chem.* 80 (1958) 5059.
- [81] G. Nurk, A. Jänes, K. Lust, E. Lust, *J. Electroanal. Chem.* 515 (2001) 17.
- [82] E. Lust, A. Jänes, K. Lust, J. Ehrlich, *Russ. J. Electrochem.* 32 (1996) 597.
- [83] S. Amokrane, J.P. Badiali, *J. Electroanal. Chem.* 266 (1989) 21.
- [84] S. Amokrane, J.P. Badiali, in: R.E.White, J.O'M. Bockris, B.E. Conway (Eds.), *Modern Aspects of Electrochemistry*, vol. 22, Plenum Press, New York, 1991, p. 1.
- [85] W.R. Fawcett, *J. Electroanal. Chem.* 500 (2001) 264.
- [86] W.R. Fawcett, D.J. Henderson, *J. Phys. Chem.* 104 (2000) 6837.
- [87] D. Boda, K.Y. Khan, D. Henderson, *J. Chem. Phys.* 110 (1999) 5346.

9. SUMMARY IN ESTONIAN

Peroksodisulfaataniooni elektrokeemiline redutseerumine Bi elektroodil

Antud töös uuriti peroksodisulfaatanioonide elektrokeemilist redutseerumist elektrokeemiliselt poleeritud Bi(111) ja Bi(01 $\bar{1}$) monokristalli tahul. Elektrokeemilise redutseerumise mehhanismi ja kineetiliste parameetrite määramiseks kasutati tsüklilist voltamperomeetriat ja pöörleva ketaselektroodi meetodit. Leiti, et S₂O₈²⁻ aniooni redutseerumisprotsessi kiirus sõltub nii S₂O₈²⁻ anioonide kui ka foonelektrolüüdi kontsentratsioonist, samuti foonelektrolüüdi keemilisest loomusest ning elektroodi potentsiaalidest. Foonelektrolüüdina kasutati NaF ja Na₂SO₄ vesilahuseid. Veel leiti, et peroksodisulfaatanioonide redutseerumise kineetiliste parameetrite väärtus sõltub Bi elektroodi pinnatöötlustest, st. Bi pinna nanoskoopilisest karedusest. Null-laengupotentsiaali all on reaktsiooni limiteerivaks staadiumiks difusioon. Potentsiaali nihkumisel negatiivsemate pinnalaengute suunas toimub S₂O₈²⁻ anioonide redutseerumise pidurdumine, mis on tingitud negatiivselt laetud peroksodisulfaatanioonide tõukumisest negatiivselt laetud Bi(*hkl*) elektroodi pinnalt. Samuti leiab aset S₂O₈²⁻ või reaktsiooni vaheühendite adsorptsioon, mis viib elektroodi pinna blokeerumisele ja seega reaktsiooni kiiruse vähenemisele.

Kineetiliste voolude leidmiseks kasutati Koutecky-Levich'i sõltuvusi. Kineetiliste voolude alusel leitud S₂O₈²⁻ aniooni redutseerumisreaktsiooni kiiruskonstant, mida pole parandatud elektrilise kaksikkihi ehitust arvestava elektrostaatilisest töö komponendiga, sõltub foonelektrolüüdi kontsentratsioonist.

Kasutades erinevaid lähendusvalemite koostatud nn parandatud Tafeli sõltuvused, kus arvestatakse elektrilise kaksikkihi ehitust. Parandatud Tafeli sõltuvuste tõusudest leitud ülekandekoefitsendi väärtused on märgatavalt väiksemad kui 0.5 ning sõltuvad suhteliselt vähe foonelektrolüüdi kontsentratsioonist. Väga väikesed ülekandekoefitsendi väärtused viitavad asjaolule, et tõenäoliselt on tegemist aktivatsioonienergiata laenguülekanne mehhanismiga. Kõige paremini langevad parandatud Tafeli sõltuvused kokku eeldusel, et reaktsiooni astuva osakese kaugus välisest Helmholtzi tasandist sõltub pöördvõrdeliselt foonelektrolüüdi kontsentratsioonist.

Keemiliselt söövitatud Bi(111) elektroodi jaoks, mille pind on nanoskoopiliselt väga kare, konstrueeritud parandatud Tafeli sõltuvuste interpreteerimine on väga komplitseeritud ning seega ei saa antud andmeid kasutada reaktsioonimehhanismi detailsemaks kvantitatiivseks analüüsiks.

10. ACKNOWLEDGEMENTS

The present study was performed at the Institute of Physical Chemistry of the University of Tartu. The support received from the Estonian Science Foundation under Project Nos. 4568, 5803 and 6455.

I wish to express my greatest gratitude to my doctoral advisors Professor Enn Lust for continuous support, scientific and general advice.

I am very thankful to Dr. Karmen Lust for collaboration in handling the computers and programs and to S. Kallip and V. Grozovski for the *in situ* STM images for electrochemically polished and chemically etched Bi(111) electrodes.

Also I would like to thank all my friends and colleagues for helpful discussions and continuous support, but my special thanks to my parents, husband and children for their support and patience.

This issue is dedicated to memory of my grandmother.

